

**PHENIX Beam Use Proposal
for RHIC Run-10 and Run-11
June 2, 2009**

The PHENIX Collaboration

1 Summary

The PHENIX Collaboration proposes a scientific program of precision measurements to pursue key goals in the study of heavy ion collisions and the spin of the proton using RHIC. We seek to quantify the properties of the perfect QCD liquid, discover the conditions under which those properties are first manifested, and take first steps in a beam energy scan with the ultimate goal of searching for evidence of the QCD critical end point. The RHIC Spin program seeks to answer the enduring puzzle of how the nucleon's half integer spin is carried by its partonic constituents. Our proposed program to develop and accumulate data on polarized proton collisions at 500 GeV will extend the x range of sensitivity to gluon polarization. We expect to have much better uncertainties; more especially, these data will have a powerful effect on global fits of the flavor dependent anti-quark polarization. In addition to quantifying the surprising properties of both hot and cold QCD matter discovered in early RHIC runs, the program proposed by PHENIX also addresses new scientific questions raised by the RHIC data from Runs 1-9. Our plan is designed to take maximum advantage of enhancements of both the PHENIX experiment and the RHIC collider as they become available.

The PHENIX detector was optimized for precision measurements of rare probes of partonic matter and polarized protons, with particular focus on hard and electromagnetic probes. PHENIX possesses selective triggers, high rate capability, and multiple fast detector systems to track and identify particles. The initial PHENIX design already foresaw luminosity beyond design values. Consequently PHENIX kept up with incremental RHIC increases via modest data acquisition improvements; the addition of stochastic cooling does, however, mandate a more significant DAQ/Trigger upgrade.

PHENIX is currently in the midst of an ambitious upgrade program. 2010 will be the final year of operations with the Hadron Blind Detector. Beginning in 2011, the new silicon microvertex barrel detector (VTX) will be available, and will be extended by the forward vertex detector (FVTX) a year later. We are currently optimizing the design of a forward calorimeter (FOCAL) to trigger on neutral pions and photons, and provide coincidence measurements with particles detected in the existing high resolution midrapidity detectors. We look forward to using these detectors and the increased luminosity afforded by stochastic cooling to investigate the proton's spin, gluon structure of the nucleus, and properties of hot, dense partonic matter with rare probes that have been previously un-

available at RHIC. We present here a program that is carefully planned to utilize these capabilities as they become incrementally available.

The requested heavy ion running will extend measurements of hard processes and electromagnetic probes from qualitative to truly quantitative. The new detector subsystems will allow heavy quark spectroscopy. Increased luminosity will allow extending the kinematic range of pion, direct photon, quarkonia, and photon-jet correlation probes. A new theme from Run-10 onward is running at lower energies to search for the onset of opacity and flow characteristic of the perfect liquid, probe in-medium hadron modification and thermal radiation via dileptons, and to look for experimental signals of the critical point of the QCD phase transition. Substantial data sets with full energy Au+Au are requested in both Run-10 and Run-11. These large data sets with new detector capabilities are crucial to maintain the excitement of RHIC program in the era of heavy ion collisions at the LHC.

p+p collision data for dielectron comparison is currently being collected in Run-9. Additional 200 GeV p+p and eventually d+Au data will be required later, once the VTX and FVTX are installed. Full exploitation of these new detector systems will be enhanced by the increased RHIC luminosity and enhanced data acquisition and triggering capabilities in PHENIX. Improved polarization and luminosity, as well as spin-flip hardware to control systematic uncertainties are key for success of the RHIC spin program.

The PHENIX Collaboration considers it imperative to maintain the vitality of the RHIC spin program by continued regular machine development and data taking. This is particularly true in light of new experimental opportunities at other facilities. We are at the dawn of an era where RHIC data provide substantial constraints to global analyses of the spin structure of the proton. Timely development of 500 GeV polarization and collection of a substantial data set is requested as well as reach lower x for ΔG .

The priorities for the PHENIX Collaboration in Run-10 are:

1. Collect data with 200 GeV Au+Au collisions, utilizing the Hadron Blind Detector to reject Dalitz decays and conversion electrons. As the Hadron Blind Detector and the Reaction Plane Detector cannot coexist with the silicon vertex detector, it is imperative to collect data with the HBD in Run-10.
2. Begin an energy scan, focusing first between full and injection energies. The goal of this scan is two-fold:
 - i Exploit the unique opportunity to investigate dielectron production in a completely new collision energy regime. Utilization of the HBD to reject background allows carrying out this measurement with 50 Million events, greatly reducing the required running time. With the HBD, dielectron production can be studied at 39 and 62.4 GeV.

- ii Search for the onset of perfect liquid properties via opacity and flow measurements, and look for possible evidence of the QCD critical endpoint at modest baryochemical potential.
3. Devote a period of approximately 5 weeks to p+p collisions. We request that up to 4 weeks be used for machine development studies aimed at improving the proton polarization in 250 GeV beams. This machine development time is key to the success of the spin program from 2011 onwards and is very important. The remaining week should be devoted to unpolarized proton-proton collisions at 22.4 GeV to serve as reference for the existing Cu+Cu data at that energy.

The priorities for the PHENIX Collaboration in Run-11 are:

- A Record 50 pb^{-1} of 500 GeV polarized p+p collisions. This can be accomplished in 10 weeks, and will allow first measurement of the W asymmetries and extend measurement of ΔG to lower x . Once collisions are established and beam-related backgrounds have been controlled, the p+p collisions will be used to commission the VTX detector.
- B Full energy Au+Au collisions for the heavy quark physics program of that vital upgrade. Furthermore, this data set, when combined with Run-7 and Run-10, will allow definitive measurement of the magnitude of J/ψ elliptic flow.

2 Introduction

The goals of the PHENIX Collaboration for RHIC running have been clearly delineated in our previous Beam Use Proposals and presentations to the Program Advisory Committee[1, 2, 3, 4, 5, 6, 7, 8, 9, 10, 11]. The consistent theme is the need for the highest possible integrated luminosities (and polarizations in the case of p+p running) to explore fully the range of fundamental phenomena in nucleus+nucleus, “proton”+nucleus and proton+proton collisions. The requested program has been designed to provide incisive measurements necessary to understand the spin structure of the proton and the nature of nuclear matter at the extremes of temperature and density, while performing the necessary baseline measurements for both the spin and the heavy ion programs.

PHENIX possesses selective triggers, high rate capability, and multiple fast detector systems to track and identify particles. Over the past years, PHENIX triggering, data acquisition, archiving, and data analysis approaches were able to keep up incremental RHIC increases via normal operational capital expenditures. However, keeping the PHENIX data acquisition and triggering capabilities matched to the increased luminosity expected in 2012 and increased data volume from new upgrades requires a more significant

DAQ/Trigger upgrade. We have been extremely successful in providing timely analysis of our data-sets using not only the RHIC Computing Facility (RCF), but also computing resources from PHENIX institutions, particularly in Japan (“CC-J”) and France (“CC-F”).

PHENIX is currently in the midst of an ambitious upgrade program. 2010 will be the final year of operations with the Hadron Blind Detector. Beginning in 2011, the new silicon microvertex barrel detector (VTX) will be available, and will be extended by the forward vertex detector (FVTX) a year later. We are currently optimizing the design of a forward calorimeter (FOCAL) to trigger on neutral pions and photons, and provide coincidence measurements with particles detected in the existing high resolution midrapidity detectors. We look forward to using these detectors and the increased luminosity afforded by stochastic cooling to investigate the proton’s spin, gluon structure of the nucleus, and properties of hot, dense partonic matter with rare probes that have been previously unavailable at RHIC.

PHENIX has made significant progress in both the heavy ion and the spin programs despite curtailed running time in each of Runs 6 through 8. Nevertheless, the missing weeks do add up, creating a backlog of integrated luminosity for both programs. The lack of running is immediately notable in the spin program, which has its first substantial operations since Run-6, is currently in progress. Although the recently completed exploratory run at 500 GeV was very successful, the overall polarized proton performance in Run-9 underscores the deleterious impact that lack of polarized p+p running has upon polarization and luminosity development. Polarization is a key factor in the figure of merit for the spin physics goals, and the expected polarization levels have not yet been attained. This significantly slows progress toward the goals laid out in the RHIC Spin Research plans[12, 13].

3 Status of the PHENIX Experiment

The PHENIX detector has evolved from a partial implementation of only the central arms in Run-1, a completed installation of the baseline + AEE (Additional Experimental Equipment) systems for Run-3, to a significantly enhanced detector from Run-4 onward. Upgrades added for Run-7 include a time-of-flight detector in the West arm, an improved resolution Reaction Plane Detector, Muon Piston Calorimeters on both the North and South side, and an initial implementation of the Hadron Blind Detector. The first three were used for physics in Run-7, while the Hadron Blind Detector was removed and repaired. It is now working well and taking data in Run-9. Additional strategic upgrades are either under construction, or nearing construction start.

Table 1: Summary of the PHENIX data sets acquired since RHIC Run-1. All integrated luminosities listed are *recorded* values.

Run	Year	Species	$\sqrt{s_{NN}}$ (GeV)	$\int L dt$	N_{Tot}	p+p Equivalent	Data Size
01	2000	Au+Au	130	1 μb^{-1}	10M	0.04 pb^{-1}	3 TB
02	2001/2002	Au+Au	200	24 μb^{-1}	170M	1.0 pb^{-1}	10 TB
		p+p	200	0.15 pb^{-1}	3.7G	0.15 pb^{-1}	20 TB
03	2002/2003	d+Au	200	2.74 nb^{-1}	5.5G	1.1 pb^{-1}	46 TB
		p+p	200	0.35 pb^{-1}	6.6G	0.35 pb^{-1}	35 TB
04	2004/2004	Au+Au	200	241 μb^{-1}	1.5G	10.0 pb^{-1}	270 TB
		Au+Au	62.4	9 μb^{-1}	58M	0.36 pb^{-1}	10 TB
05	2004/2005	Cu+Cu	200	3 nb^{-1}	8.6G	11.9 pb^{-1}	173 TB
		Cu+Cu	62.4	0.19 nb^{-1}	0.4G	0.8 pb^{-1}	48 TB
		Cu+Cu	22.5	2.7 μb^{-1}	9M	0.01 pb^{-1}	1 TB
		p+p	200	3.8 pb^{-1}	85G	3.8 pb^{-1}	262 TB
06	2006	p+p	200	10.7 pb^{-1}	230G	10.7 pb^{-1}	310 TB
		p+p	62.4	0.1 pb^{-1}	28G	0.1 pb^{-1}	25 TB
07	2007	Au+Au	200	0.813 nb^{-1}	5.1G	33.7 pb^{-1}	650 TB
08	2008	d+Au	200	80 nb^{-1}	160G	32.1 pb^{-1}	437 TB
		p+p	200	5.2 pb^{-1}	115G	5.2 pb^{-1}	118 TB
09	2009	p+p	500	≈ 10 pb^{-1}	308G	≈ 10 pb^{-1}	223 TB
		p+p	200	ongoing			>220 TB

Table 1 summarizes the data collected in Runs 1-8, and in Run-9 so far. For each data-set the “*proton+proton equivalent*” “*recorded*” integrated luminosity is given by the corresponding column of the table. For an $A+B$ collision the *proton+proton equivalent* integrated luminosity is given by $\int \mathcal{L} dt|_{p+pequivalent} \equiv A \cdot B \int \mathcal{L} dt|_{A+B}$, which corresponds to the integrated parton+parton luminosity, without taking into account any nuclear enhancement or suppression effects. The *recorded* integrated luminosity is the number of collisions actually examined by PHENIX, as distinguished from the larger value delivered by the RHIC accelerator. In the case of minimum bias data sets, “*recorded*” is strictly accurate, while for triggered data “*sampled*” more accurately describes the process. We use “*recorded*” as shorthand for either case to refer to the number of events examined by PHENIX for a given physics observable

Between mid-2008 and the present time, PHENIX submitted ten new papers for publication. arXiv:0903.3399[14] is the first publication on direct photon-jet correlations at RHIC; the measurement is done using leading hadrons from the jet and unfolding the direct photon triggered correlations from the inclusive photon triggered correlations in both p+p and Au+Au collisions. As the photon energy tags the energy of the jet, this is a long awaited “golden channel” to study medium induced energy loss and the resulting modification of the parton fragmentation at RHIC. We find that the direct photon associated yields in p+p collisions scale approximately with the momentum balance, $z_T = p_T^{hadron}/p_T^{photon}$, as expected for a measure of the away-side parton fragmentation function. In Au+Au, on the other hand, associated particles are suppressed at a level that is comparable to that observed for high p_T single hadrons and dihadrons. This indicates surface bias toward the hadron emission side of the system. Preliminary results from Run-7, shown in Figure 1, were presented at Quark Matter 2009 in April; the higher statistical precision and kinematic reach indicate steepening of the Au+Au fragmentation function, as expected from medium-induced energy loss.

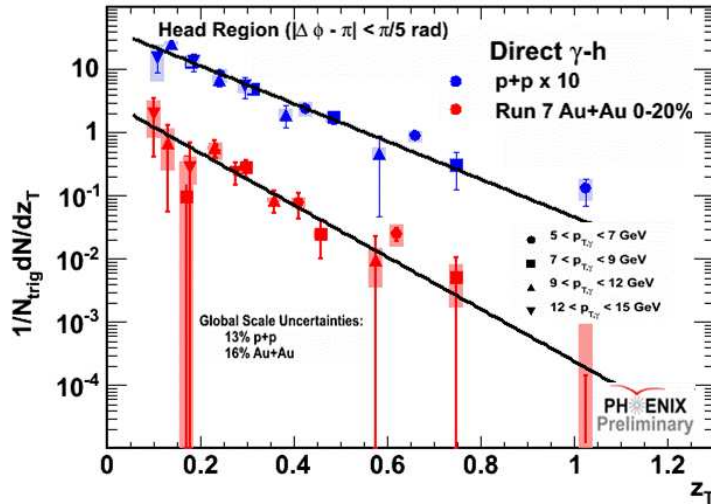


Figure 1: Fragmentation function $z_T = p_T^{hadron}/p_T^{photon}$, measured by $\gamma_{direct} - h$ coincidence in p+p and Au+Au $\sqrt{s_{NN}} = 200$ GeV.

Together with a new PHENIX publication reporting on the reaction plane dependence of high p_T hadron suppression[15], these results provide important constraints to calculations of different energy loss mechanisms. Another new publication presents the first separation of c and b quark at RHIC, utilizing non-photonic electron-hadron correlations in p+p collisions at $\sqrt{s} = 200$ GeV[16]. The extracted c and b production cross sections agree with those inferred from dileptons in [17]. With these papers, PHENIX enters the era of using rare probes to ascertain properties of the hot partonic medium. These first results also demonstrate, though, the need for increased luminosity, precision particle identification, improved trigger rejection and data acquisition capability, as well as enhanced acceptance in order to fully engage in precision measurements.

Two papers from the spin run in 2006 were completed. High $x_{Bjorken}$ of the gluon was probed for the first time at RHIC via π^0 production in 62.4 GeV polarized proton collisions.[18], and we presented greatly improved measurements of the double helicity asymmetry in neutral pion production at $\sqrt{s} = 200$ GeV in Ref. [19]. The measured asymmetries are consistent with zero, and provide constraints on global fits on the positive ΔG side. This can be seen in Figure 2 and in [20]. Again, the data demonstrate the importance of significant running time with high luminosities and polarizations if RHIC is to solve the mystery of the gluon spin.

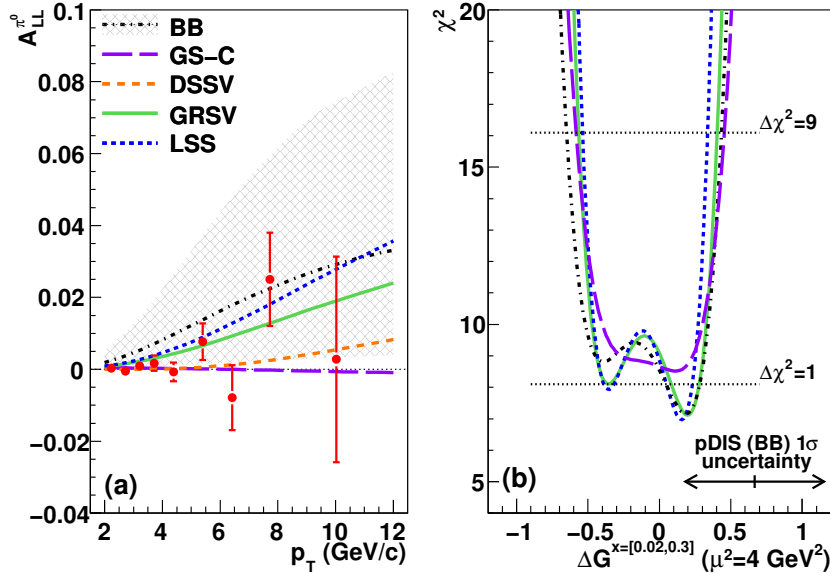


Figure 2: left: π^0 asymmetry expectations for different $\Delta g(x)$. Hatched band is the pDIS uncertainty (BB). Points are the combined Run-5 and Run-6 results. right: The χ^2 profile as a function of $\Delta G^{[0.02,0.3]}$ for the same parameterizations. Arrows indicate 1σ uncertainty on BB best fit. $\Delta\chi^2$ values are shown for GRSV.[21]

We have reported first measurements of thermal photon emission, from which the initial temperature can be inferred with the aid of hydrodynamical models[22]; this temperature lies between about 300 and 600 MeV, depending on how early thermalization is achieved. Other papers report correlation[23] and fluctuation[24] measures of the bulk medium, as well as systematic studies of the elliptic flow measured in several different ways to control systematic uncertainties[25]. Our studies of the bulk represent an important step toward developing methodologies for a phase transition search. This is discussed below.

3.1 Achievements in Run-7

The configuration of PHENIX starting in Run-7 is shown in Figure 3. Not visible in this figure are the new muon trigger components which were partially installed for Run-9.

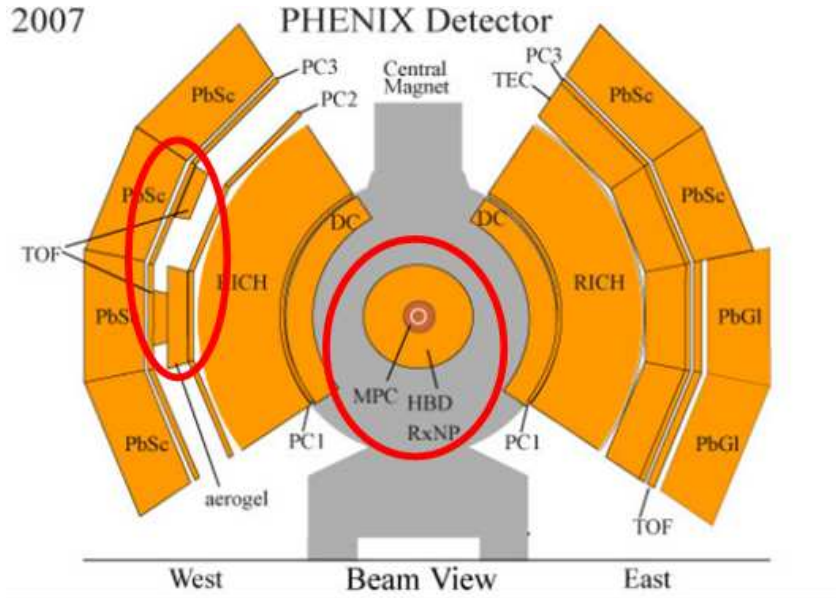


Figure 3: Configuration of PHENIX for 2007 and 2008, showing the location of the Reaction Plane Detector (RXNP), Time of Flight-West (TOF-W), Hadron Blind Detector (HBD) and the Muon Piston Calorimeter (MPC).

The Au+Au data set collected in Run-7, and utilizing the TOF-W, RXNP and MPC detectors, exceeded our previous statistics by nearly a factor of 4. Reconstruction of the Run-7 data was completed approximately a year ago, and preliminary results have been shown at the Quark Matter conferences in 2008 and 2009. Several papers on these results are in preparation

A number of new physics insights were found by PHENIX from the Run-7 data, in addition to those discussed above. A number of these utilize the new detector subsystems. The list includes:

- Quark number scaling of elliptic flow is broken at p_T per quark above 1 GeV/ c . The location of this point and its centrality dependence depend on the viscosity of the parton liquid.
- Scaling works for v_4 just as well as for v_2 ; $v_4 = k(v_2)^2$ independently of PID.
- Heavy quarks flow to at least 5 GeV/ c , where the contribution of single electrons from B meson decays should become significant. This surprising result utilizes the improved reaction plane resolution of the RXNP detector.

- For dijet probes of the medium, the away side yields drop from in-plane to out-of-plane. This indicates that the medium is “gray” rather than completely opaque to jets.
- The strongly modified structure of away-side jets in Au+Au collisions has a reaction plane dependence that is very different from that of the jets that punch through.
- The spectrum of particles in the two particle correlation near side “ridge” is harder than the bulk, and in fact very similar to that in the modified jet on the away-side.
- Υ is suppressed in central Au+Au collisions.

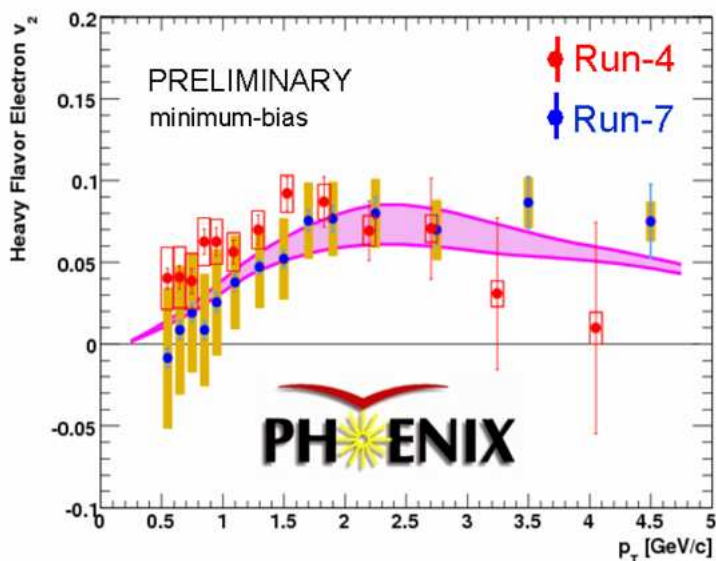


Figure 4: Left-hand figure: Identified hadron v_2 and v_4 measurements vs p_T in mid-central collisions. Right-hand photo: b) v_2 of non-photonic electrons; the dominant source of such electrons is the decay of D and B mesons. The blue points indicate the Run-7 data, and show that substantial elliptic flow is observed even for heavy quarks.

3.2 Achievements in Run-8

The d+Au data collected in Run-8 is a factor of 30 larger than that available from the last d+Au run in 2003. Over 80 pb^{-1} of integrated luminosity was sampled, representing 160 billion minimum-bias events. Reconstruction was completed at the beginning of this year and analysis of this data is now underway with a several new results presented at Quark Matter 2009.

This data set will provide a much needed reference for cold nuclear matter effects on probes of the hot, dense matter produced at RHIC. In particular it will provide the following:

a) the level of suppression relative to p+p collisions of J/ψ and heavy quark production to understand the effects due to a modification of the structure functions (shadowing), energy loss in ordinary matter, and the absorption (breakup cross section) of the J/ψ in the final state. The data will serve to identify and quantify the magnitude of suppression seen in Au+Au collisions which can be attributed to hot matter effects.

b) a precision measurement of direct photons at high transverse momentum to serve as a baseline for direct photon production in Au+Au collisions.

c) a quantification of the Cronin effect in the central arm by using the TOF-West and Aerogel counters, (not available in Run-3) for particle identification at high p_T . The extent to which the baryon enhancement in d+Au exceeds the meson enhancement, along with possible saturation of the enhancement with the number of nucleon-nucleon collisions, will allow PHENIX to solve the several decade long mystery of whether the Cronin effect is due to initial state multiple scattering in the target nucleus.

d) a search for evidence of saturation of gluons in nuclei at small momentum fraction using the Muon Piston Calorimeters (MPC) in place during Run-8. This will be done both by looking at R_{dAu} and correlations between the MPCs and the central arm data.

Because of its short duration, low polarization, low luminosity, and lack of radial polarization development, the p+p running in Run-8 allowed PHENIX only to double the modest-sized transverse polarized p+p statistics from Run-6. Nevertheless, we will combine the two data samples and study the interference fragmentation function, Siverts effect and A_N in transversely polarized proton-proton collisions. In particular, the MPC's now allow PHENIX to study transverse spin effects at forward rapidities, where such effects are often larger.

3.3 Achievements in Run-9

- 500 GeV test run; background measurement and W observation
- Measurement of J/ψ and Υ in 500 GeV p+p collisions
- HBD commissioning and comparison run with 200 GeV p+p
- MuTrigger test run & commissioning of MuTr FEE trigger

3.4 Hadron Blind Detector

The Hadron Blind Detector (HBD) is a novel proximity focused Cerenkov detector, which is insensitive to most charged hadrons created in the central rapidity region. The HBD's novel readout technology utilizes a stack of three GEM detectors with a CsI photocathode deposited on the top GEM. Essentially all electrons from Dalitz decays and conversions are detected, allowing rejection of the majority of pairs that form the combinatorial background to low-mass e^+e^- pairs. Reduction of this background is crucial to high quality measurement of dielectron signals of thermal radiation, chiral symmetry restoration and medium modifications to hadron properties. Results from Run-4, shown below, indicate an excess of low mass dielectrons in central Au+Au collisions. The current result is obviously limited in both statistics and systematics by the very small signal-to-background ratio. The background rejection provided by the HBD is essential to obtain quantitative results.

3.4.1 HBD Commissioning in Run-9

Run-7 was the first run in which the HBD was installed, and served as an engineering run for this new detector technology. During the run, a problem was discovered with the high voltage system that resulted in releasing more than the expected amount of stored energy during a discharge, causing damage to many of the GEMs. In addition, a flaw was found in the firmware of the LeCroy High Voltage modules (1471N) which briefly re-applied high voltage to the GEMs after a trip. One half of the HBD was operated during Run-7, and the entire HBD was rebuilt in 2008. Many GEMs were successfully recuperated by washing with deionized water, which is a routine operation at the end of the regular production of GEM foils. We have improved the protection against discharges by modifying the resistive chain powering scheme and have fixed the problem with the Lecroy HV modules. Furthermore, we improved the assembly procedure, under much cleaner conditions.

The rebuilt HBD is currently in operation in PHENIX, and data collected in the initial week of running has been analyzed. While the 500 GeV polarized proton data was collected with the central magnet field in the ++ mode, the 200 GeV run underway utilizes the +-, or bucked field, configuration which put zero magnetic field at the HBD. As of this writing, insufficient 200 GeV data have been analyzed to determine the overall hadron rejection factor. However, the preliminary analysis available so far reveals improved performance compared to that obtained in the commissioning during Run-7. The improvement is close to that anticipated last year. We observe 20 photoelectrons for each electron traversing the HBD.

Figure 5 shows the matching and charge distribution of single electron tracks. This study is done using two identified electrons in the central arms with mass $m < 150 \text{ MeV}/c^2$

matched to two separate clusters in the HBD. The top two panels show the distribution of residuals between identified electron tracks and hits in the HBD along the ϕ (azimuthal angle) and z (along the beam) axes. The matching resolution both in z and ϕ is $\sigma_z \approx \sigma_\phi \approx 1$ cm, which is determined by the HBD hexagonal pads of size $a = 1.55$ cm ($2a/\sqrt{12} = 0.9$ cm). The lower left panel shows the charge in the HBD, calibrated into photoelectrons, for matched single tracks identified as electrons using the RICH and EMCAL. There is a clear peak at 20 photoelectrons. The lower right plot shows the number of fired pads in the HBD that correspond to these tracks.

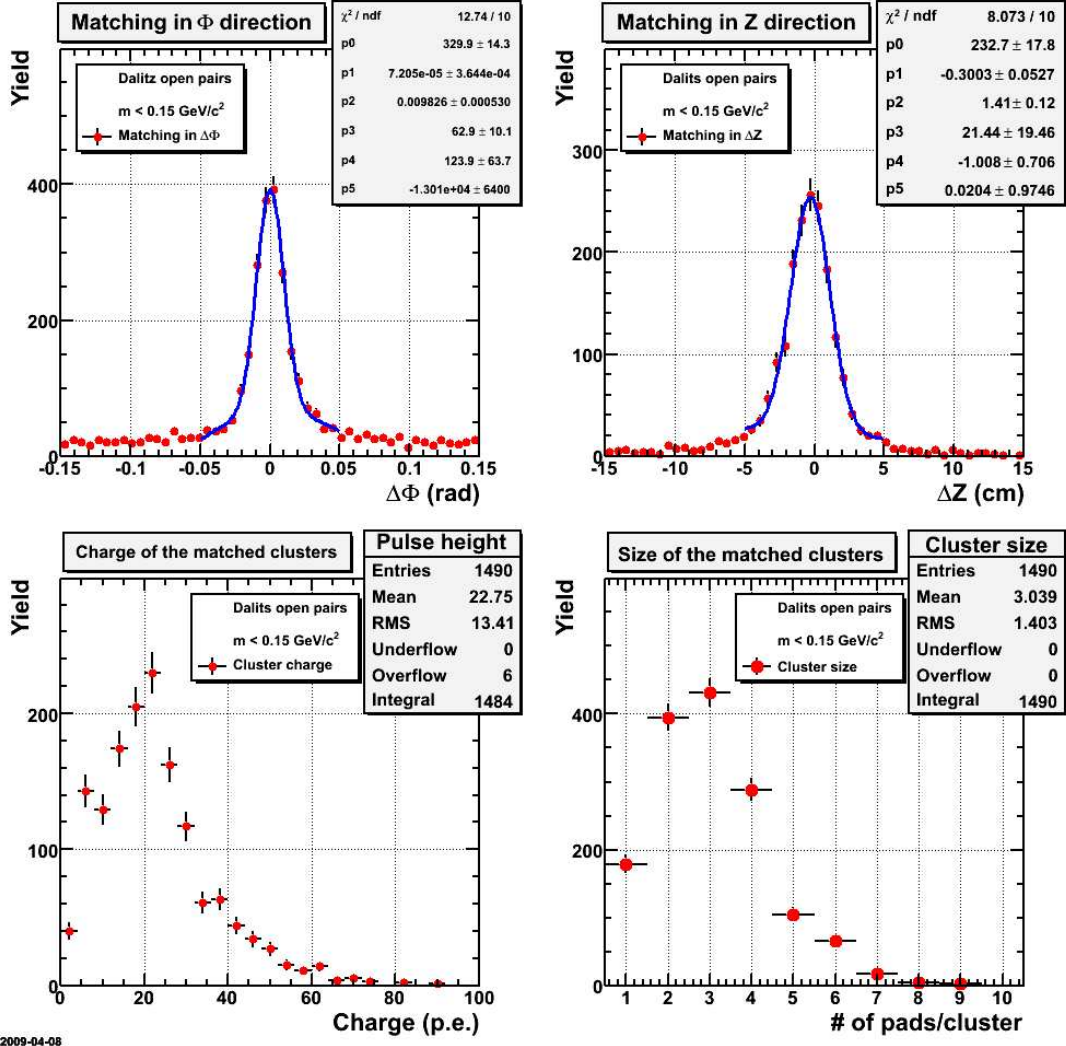


Figure 5: Top: Matching distributions in ϕ (azimuthal angle) and in Z (along the beam axis) of single electrons to the HBD. Bottom: HBD response in number of photoelectrons (left) and cluster size (right) to single electrons.

Figure 6 shows the matching and charge distribution of double electron tracks. In this study, the two identified electrons in the central arms with $m < 150$ MeV/ c^2 matched to

a single cluster in the HBD. It is clear that the matching in this case works similarly to that for single tracks, while the number of photoelectrons, peaked at 40, is double that of the single tracks. The values for single and double electron response allow us to project the performance in Au+Au collisions, which is discussed below.

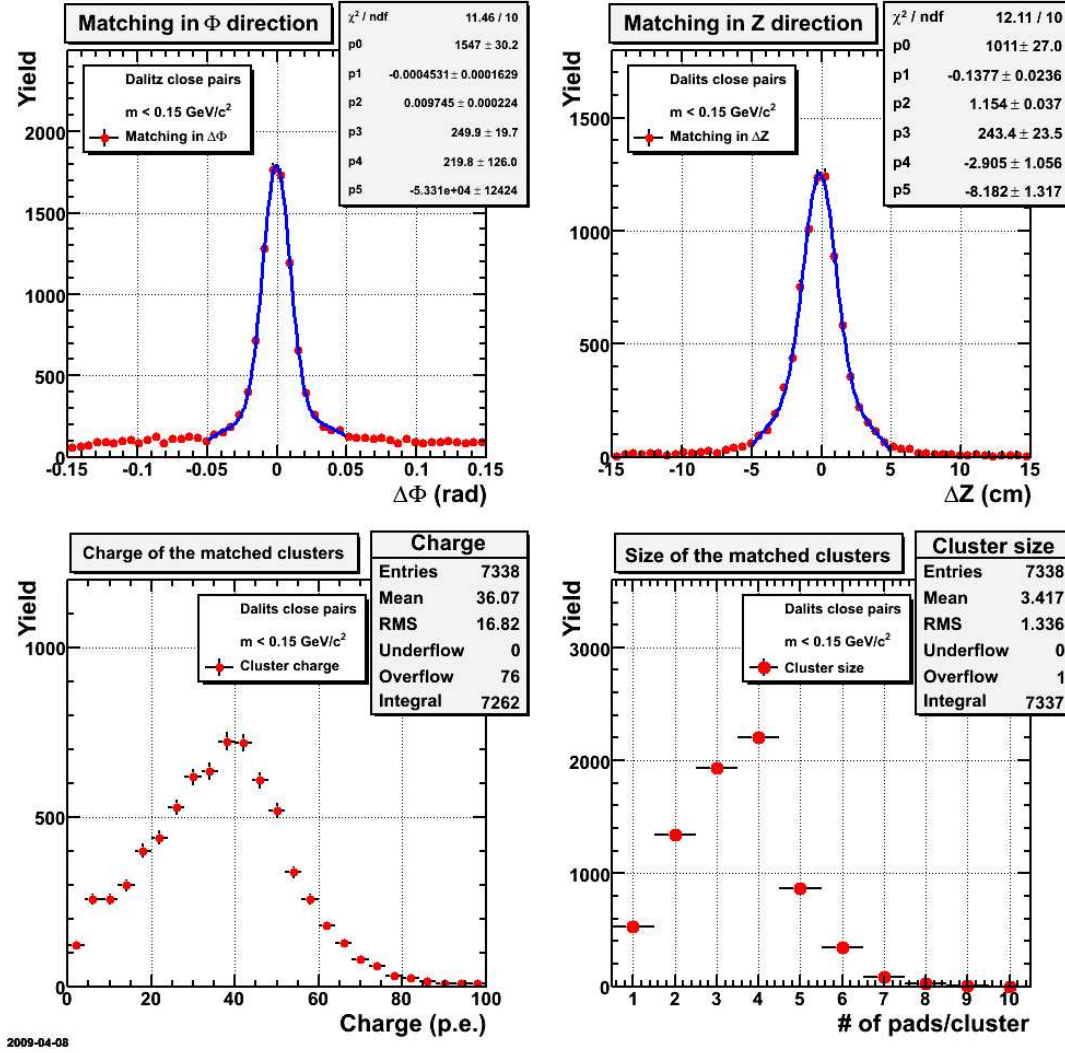
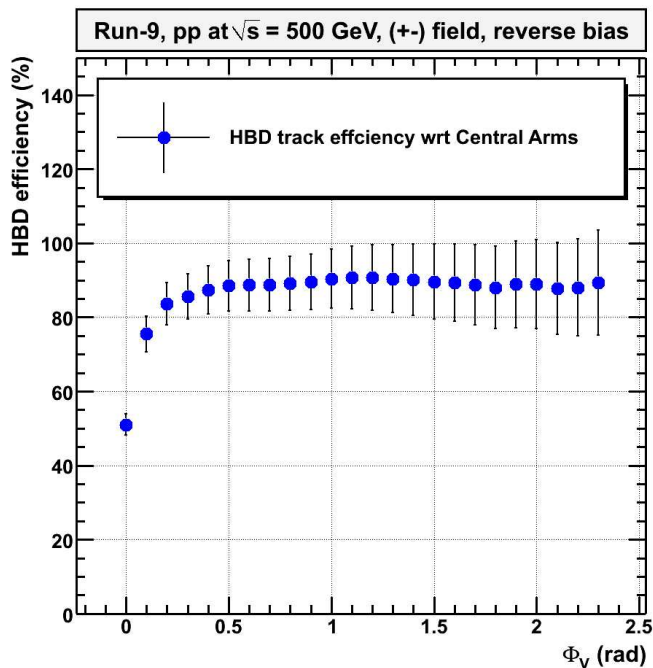


Figure 6: Top: Matching distributions in ϕ (azimuthal angle) and in Z (along the beam axis) of two electrons matched to a single cluster in the HBD. Bottom: HBD response in number of photoelectrons (left) and cluster size (right) to double electrons.

The single electron efficiency of the HBD was derived from a sample of open Dalitz decays, and is shown in Figure 7 as a function of opening angle of the track pair. Preliminary analysis of the J/ψ using the electron triggered data sample confirms that the single electron detection efficiency is close to 90% in the HBD.

Evaluating the hadron blindness of the HBD will require analysis of a larger data set



2009-05-27

Figure 7: HBD single electron track efficiency with respect to the central arms for Run-9 $p + p$ collisions at $\sqrt{s} = 500$ GeV.

than has currently been scanned. However, the data from Run-7 allow a first glimpse; the true performance will be considerably better as the electron response is now 20 photoelectrons, much larger than the ≈ 14 photoelectrons achieved in Run-7. The left panel in Figure 8 demonstrates the suppression of the hadron response of the detector in reverse bias mode as compared to the forward bias case. The middle panel shows the electron-hadron separation in reverse bias mode. Adequate hadron rejection is achieved with a simple amplitude cut, as shown on the right panel. Hadron rejection factors in excess of 100 are obtained by combining the the amplitude cut with a cluster size cut, since hadrons produce single pad clusters whereas single electrons typically produce clusters of 2-3 pads.

The expected background rejection by the HBD can be estimated based upon the analysis of the Run-7 data, and correction for the improved response. The projections for S/B improvement are discussed below, in the heavy ion physics section. The Run-7 analysis is shown here for completeness. The left panel in Figure 9 shows the invariant mass spectrum in the PHENIX east central arm, within the same acceptance of the HBD east that was operational in Run-7. This is the spectrum prior to any rejection of the combinatorial background using HBD information. The middle panel shows the same spectrum after applying HBD rejection utilizing the cuts described above. In both panels the red points represent the measured unlike sign spectrum and the blue points show the

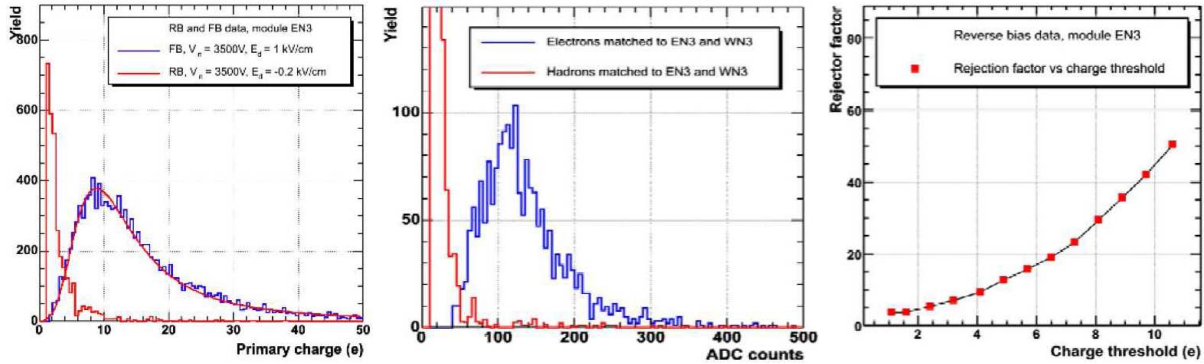


Figure 8: Left panel: hadron suppression illustrated by comparing hadron spectra in forward bias (FB in blue) and reverse bias (RB in red). Middle panel: electron-hadron separation in RB. Right panel: hadron rejection factor as function of the cut on the charge signal.

properly normalized combinatorial background determined by a mixed event technique. The right panel shows the net signal (unlike spectrum - combinatorial background) after HBD background rejection cuts. This is an ongoing analysis based on less than 10% of the available statistics and restricted to events with centrality $< 50\%$. The present results include only the HBD benefits from matching, double hit rejection and partial rejection of conversions in the radiator gas. The close hit cut and the cluster size cut are not applied, as they will be different for the final HBD. Monte Carlo studies indicate that these cuts should improve the combinatorial rejection power of the HBD. Even with the incomplete analysis of Run-7 data, the benefit of the HBD is apparent. The signal, as monitored by the π^0 Dalitz yield (with $m < 150 \text{ MeV}/c^2$), remains basically unchanged, whereas the combinatorial background is considerably reduced, resulting in an improvement of the S/B ratio by almost an order of magnitude for masses with $m > 150 \text{ MeV}/c^2$.

3.5 Future Upgrades for Installation Beyond Run-9

The PHENIX Beam Use Proposal is guided by the carefully structured, ongoing program of upgrades. In particular, the request is predicated on making all necessary measurements in Au+Au with the HBD in Run-10. Following that, the HBD will be removed from its data-taking position (along with the RXNP) in order to install the VTX detector, together with mechanical infrastructure to support the FVTX.

A program of substantial upgrades to the PHENIX detector has been developed to measure key observables which are either inaccessible at RHIC to date, or have been measured only with limited precision and kinematic reach. The Muon Trigger, silicon central barrel vertex detector (VTX) and forward vertex detector (FVTX) are currently under construction. Capability for forward calorimetry is needed to address key physics ques-

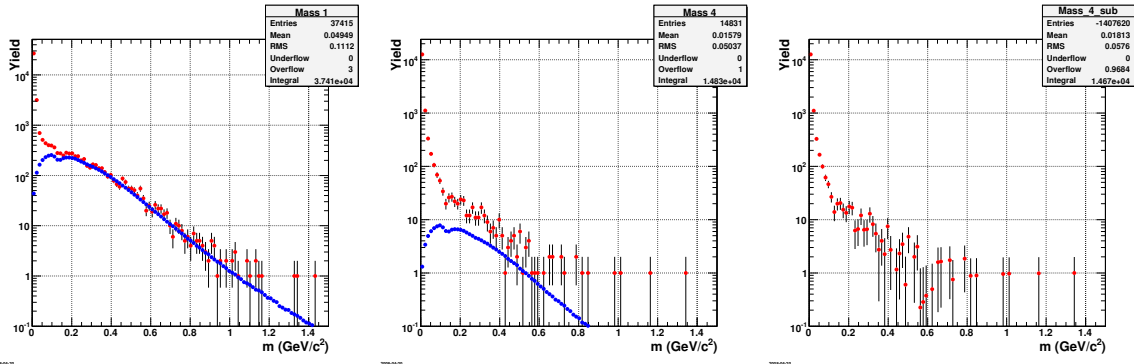


Figure 9: Invariant mass spectra before (left panel) and after partial (middle panel) background rejection cuts on HBD data. The red points represent the measured unlike sign pairs (U) and blue points the properly normalized combinatorial background (B) derived from a mixed event technique. The signal, obtained from the subtraction U-B after HBD rejection cuts, is shown in the right panel.

tions, and conceptual design of a forward calorimeter optimized for p+p and d+Au physics is underway. We envision that the detector will also be utilized in Au+Au collisions, but occupancy considerations may result in only partial rapidity coverage or resolution in central Au+Au collisions. These major upgrades address observables that are critical to advancing understanding in three physics areas accessible at RHIC: high temperature QCD via the heavy ion program, the spin structure of the nucleon, and, thirdly, the parton content of the nucleus, which can be determined in “nucleon”-nucleus collisions.

3.5.1 VTX and FVTX

Precision tracking near the interaction vertex with highly segmented silicon detectors (VTX and FVTX) is being constructed to tag products from weak decays of mesons carrying heavy quarks (charm and bottom). The primary goal is to improve the signal to background on these measurements, allow separation of charm and bottom, and provide improved mass resolution in the muon arms. The silicon detectors will be used in conjunction with the electron tracks in the central arms and muon tracks in the muon arms to measure displaced vertices and tag leptons from heavy meson and quarkonium decays. The silicon detectors also will provide the mass resolution required to study the fate of different quarkonia in the partonic matter. The J/ψ measurements will be supplemented by ψ' and χ_C to probe the extent of color screening in the medium formed at RHIC. It should be noted that the VTX, having full azimuthal acceptance, and covering a pseudorapidity range larger than the PHENIX central arms, substantially increases the PHENIX acceptance for hadrons at midrapidity. Stand-alone tracking software performance has recently been demonstrated. Consequently, the VTX will improve jet correlations measurements of various types.

First measurements at RHIC with “non-photonic” leptons show that medium effects are large and heavy flavor seems to equilibrate more rapidly than expected. This calls into question our understanding of the energy loss mechanism in the dense, hot medium created in Au-Au collisions at RHIC, particularly the role of collisional energy loss. More detailed experimental data, particularly the fate of bottom quarks, are needed. Furthermore, these new detector systems will allow PHENIX to test predictions of recent theoretical work utilizing the duality between gravity and QCD-like field theory known as AdS/CFT correspondence. These calculations[26] show how measurements of heavy flavor energy loss and flow can be used to constrain fundamental parameters like diffusion lengths or viscosity of the medium. The ratio of charm to bottom suppression can show whether perturbative QCD or AdS/CFT provide more appropriate descriptions of the energy loss mechanism[27]. In addition, heavy flavor measurements add a new channel sensitive to gluon spin contributions to the elusive spin of the proton.

The VTX is supported by both the US (DOE) and Japanese funding agencies. The inner two layers of the VTX are two planes of pixel detectors, similar to those developed in the ALICE experiment at LHC. The HBD and VTX/FVTX detectors are all located in the PHENIX central region inside the central magnet. Their installation and operation are tightly interlinked; in particular, it is not possible for the HBD and the silicon detectors to co-exist inside PHENIX. In summer 2010 the full central barrel VTX detector (VTX) will be completed and installed into PHENIX. We plan to use p+p collisions in Run-11 to commission the VTX detector, and the subsequent full energy Au+Au collisions to utilize the VTX in Run-11.

The FVTX forward silicon vertex detector endcaps are funded by the DOE, and construction is currently underway. We anticipate that this new PHENIX subsystem will be installed in summer 2011, in time for the 2012 run. A partial installation and engineering run may be possible a year earlier. As the FVTX produces physics impact by adding high resolution tracking points for muons ahead of the hadron absorber, it is utilized together with muon arm tracks. Consequently, a partial installation and successful commissioning prior to the first full run offers an excellent possibility for first physics results.

3.5.2 Muon Trigger

Measurements of parity violating spin asymmetries in W-production with the PHENIX muon arms require a first level muon trigger that selects high momentum muons, $p > 10$ GeV, and rejects the abundant muons from hadron decay, cosmic rays, and beam backgrounds. The existing muon trigger identifies muon candidates based on their ability to penetrate a sandwich of steel absorber and muon detector planes. Muons with momenta above $p > 2$ GeV are selected. The resulting trigger rejection factor varies from $200 < R < 500$, depending on the (varying) beam background levels. The muon trigger upgrade introduces tracking and timing information to the muon trigger processors. The additional

information will increase the muon trigger rejection by more than a factor 30 to $R > 6000$.

The PHENIX muon trigger upgrade has two components: (I) new front-end electronics for the muon tracking chambers to send tracking information to new dedicated muon trigger processors. This system has been developed, constructed and partially installed. (II) Two resistive plate chamber trigger detector stations, RPC-1 upstream and RPC-3 downstream, added to each muon spectrometer. The RPC stations will be used both for tracking and timing and are based on technology developed for the CMS muon trigger. The timing information adds background rejection power in offline analysis, particularly to remove tracks due to cosmic rays. Detailed Monte Carlo studies with realistic detector response and background simulations were carried out from 2006 to 2008 and have established the feasibility of the trigger upgrade. RPC detector response and electronics performance were established through a series of prototype tests.

For Run-9 the new muon tracker trigger electronics was installed in the north muon spectrometer and has been operating successfully from the beginning of the 500 GeV portion of the run. In the south, one half octant of the muon spectrometer was instrumented with the new trigger electronics and, in the same acceptance, two full-size RPC prototypes were mounted. This setup allows a full system test of the new muon trigger during Run-9.

The efficiency and noise performance of the muon tracker front-end electronics measured in Run-9 meet specification; production of the remaining electronics boards for the south muon spectrometer is presently underway. The south muon tracker trigger electronics will be installed in late summer 2009, completing the muon tracker electronics portion of the trigger upgrade.

The two full-size RPC prototypes have been successfully commissioned and are routinely read out in the PHENIX data stream. RPC hits were matched successfully with muon tracks and initial results from timing, threshold and high voltage scans are available. All parts for the RPC-3 detector stations have arrived at BNL and the assembly of RPC-3 has been started. It is estimated that the RPC-3 north station will be ready for installation in August. RPC-3 south and RPC-1 detector stations will be completed by the summer of 2010. The minimum configuration for the W-trigger in a PHENIX muon spectrometer requires all muon tracker trigger electronics and RPC-3. This configuration will be available in the Fall of 2010 in both North and South. At the highest RHIC luminosities, RPC-1 must be in place.

The muon trigger upgrade is supported through grants from the JSPS in Japan (muon tracker electronics) and the NSF (RPCs and trigger processors). The upgrade project is carried out by a group of 91 PHENIX collaborators from 19 institutions in the US, China, Korea and Japan.

A 10 member W-physics taskforce was formed in late 2008 to carry out offline analysis

of the 500 GeV portion of Run-9. The taskforce will provide feedback on the detector and upgrade performance as well as analyze the high p_T inclusive electron signal in the PHENIX central arm.

3.5.3 DAQ/TRIGGER 2010

The strategy of PHENIX has been to optimize our data acquisition system for maximum rate and design a trigger system with high rejection power and many parallel triggers. Before Run-7, PHENIX was able to record *every* minimum bias Au+Au collision. In Run-7 the Au+Au interaction rate reached 7 kHz, and PHENIX was able to record 80% of interactions (in all centralities) without triggering on specific channels or centrality. This was achieved by sustaining a 5 kHz DAQ bandwidth and an archiving rate of 750 Mbytes/second. High rates are important because it is nearly impossible to devise an effective trigger for low mass dielectrons and low p_T hadron correlations. In p+p collisions, selective Level-1 triggers reduce the 200-400 kHz interaction rates to about 6 kHz rate of useful events, which can be recorded with a livetime of approximately 90%. Thus we have been able to effectively sample the full luminosity for all rare channels.

Future RHIC runs promise interaction rates of about 7 MHz for 500 GeV p+p collisions and near 3 MHz at 200 GeV. Au+Au interaction rates will reach 40 kHz at 200 GeV, inside a vertex cut of ± 30 cm, once full stochastic cooling is implemented. Consequently, our previous strategy of recording nearly all minimum bias Au+Au interactions will not keep pace with the luminosity; selective triggering at Level-1 will be required. Furthermore, once the new silicon detectors are added, the size of each event will increase by a factor of 1.7. Studies are currently ongoing on how to increase the rejection factors of existing triggers on central arm and muon arm information. It is already clear that the EM calorimeter-based triggers will require sharpening the turn-on curves. Some of this may be achievable by better gain-matching, but reworking the now 10-year old front end electronics to reduce noise and compare fully digitized data against thresholds is also needed.

In addition, a number of small and medium scale upgrades to the data acquisition system will be made in order to maintain the event rate with larger events. For example, the central data switch and modules providing data to it will be upgraded to 10 Gigabit networking.

3.5.4 FOCAL

In order to pursue several critical physics measurements in both spin and heavy ion physics, PHENIX must extend its coverage for photons, π^0 's and jets to the forward rapidity region. This will dramatically increase the acceptance for events with a photon+jet

or two π^0 s in the final state. In p+p and d+Au such correlations constrain the kinematics of the hard collision by measuring $x_{Bjorken}$. FOCAL will extend measurement of how low-x gluons contribute to the spin of the proton into a region inaccessible with mid-rapidity measurements. In d+Au collisions PHENIX will be able to probe the nuclear gluon distributions to lower x. This is critical to pinning down the initial conditions in heavy ion collisions, and of prime interest in its own right. Shadowing or gluon saturation in heavy nuclei are under intense theoretical discussion, and require high quality new data.

Transverse spin studies also require forward calorimetry. For example, photon+ jet correlations at forward rapidity will yield an asymmetry dominated by the quark Sivers distribution. The Sivers effect displays an interesting process dependence - the sign of the asymmetry in polarized proton-proton collisions can be predicted in a kt-factorized approach to QCD, while the magnitude can be estimated from measurements in semi-inclusive deep-inelastic scattering. Measurements in PHENIX will provide a stringent test of the current theoretical framework predicting this process dependence. Another important transverse spin measurement is the Collins fragmentation function using reconstructed jets and π^0 s. Finally, in Au+Au collisions the increase in statistics and rapidity coverage for high energy photons, π^0 's and jets will make possible a much more detailed study of parton energy loss, and medium response than would otherwise be available.

The proposed FORward CALorimeter (FOCAL) is a novel, compact device composed of tungsten absorber with silicon pad readout. The coverage will be $1 < |\eta| < 3$ and 2π in azimuth and $24 X_0$ deep; it will be positioned on the front of the PHENIX muon magnets. The readout of the pads in three layers will allow the longitudinal, as well as the lateral, profile of showers to be used to reject hadronic background. In order to identify photons and π^0 's to high energy, layers of high resolution silicon strip detectors are inserted within the first several radiation lengths. FOCAL will be able to reconstruct the π^0 invariant mass to an energy of about 60 GeV.

The FOCAL is currently being designed, with a beam test of key components scheduled for summer 2009. Construction of the FOCAL will take two years, with installation planned in summer 2012.

4 Discoveries and Future Goals of the Heavy Ion Program

Heavy ion collisions at RHIC have produced striking - and very surprising - results. A dense, hot, collectively flowing medium is created, which is extremely opaque to quarks and gluons traversing it. In our White Paper, PHENIX laid out the evidence that this medium is partonic, not hadronic, in nature[28]. Discoveries since that was published further strengthen this conclusion.

4.1 Opacity, Collective Flow, and Physics of the Perfect Fluid

PHENIX has shown that even charm quarks are effectively stopped by the medium, and that they participate in the collective flow along with everything else[29]. We have made great strides in quantifying the energy loss by constraining various energy loss models with high quality data[30]. The outcome of these studies has sparked an enormous amount of theoretical work and debate in the field. It has proven difficult, though perhaps not impossible, to reproduce the observed light and heavy hadron suppression using perturbative descriptions of the energy loss. However the alternate extreme of very strong coupling is neither clearly required nor ruled out by the existing data. The role of collisional energy loss is under active study, and a unified picture that can describe the mass, centrality, p_T , reaction plane, and beam energy dependence of parton energy loss has yet to be discovered. Progress on this question requires theoretical effort, but also high precision data on light hadron and heavy flavor suppression at the highest p_T , the reaction plane dependence of energy loss, separate determination of charm and bottom energy loss, and direct photon-hadron correlation data to probe directly the medium effect upon fragmentation functions. We have begun to publish first results on many of these questions, and the needed precision measurements drive the PHENIX upgrade plan.

Another key question is under what conditions of temperature and baryochemical potential these remarkable properties exist. This motivates an energy scan in a range between top SPS and top RHIC energy.

arXiv:0801.4555[31] showed the results of a first energy scan to search for the onset of jet quenching in the hot, dense medium created in heavy ion collisions. The search was done by measuring the nuclear modification factor R_{AA} , which is the ratio of yield in ion collisions compared to that expected from the commensurate number of p+p collisions, of π^0 's at several energies. Figure 10 shows that, in Cu+Cu collisions, strong jet quenching (i.e. suppression of high momentum particle production) is observed in 200 and 62.4 GeV per nucleon pair collisions, but there is no suppression at 22.4 GeV. The presence of nuclei actually enhances particle production. This enhancement, the ‘‘Cronin effect’’ long known in collisions at several tens of GeV, may mask the presence of some energy loss of quarks and gluons in 22.4 GeV heavy ion collisions. However, the observed change from strong suppression to no suppression clearly shows that the large opacity of the hot, dense medium of quarks and gluons discovered at RHIC has an onset somewhere between 22.4 and 62.4 GeV per nucleon pair collision energy. Pinpointing at which energy jet suppression first occurs will indicate the conditions required for formation of the ‘‘perfect fluid’’.

While measurement of R_{AA} of neutral pions at high p_T will address this question, our goal is to collect sufficient data to determine other properties of the medium simultaneously. Utilization of the HBD to reject combinatorial background in dielectrons will allow PHENIX to measure the temperature of the medium, via analysis of low mass, high p_T

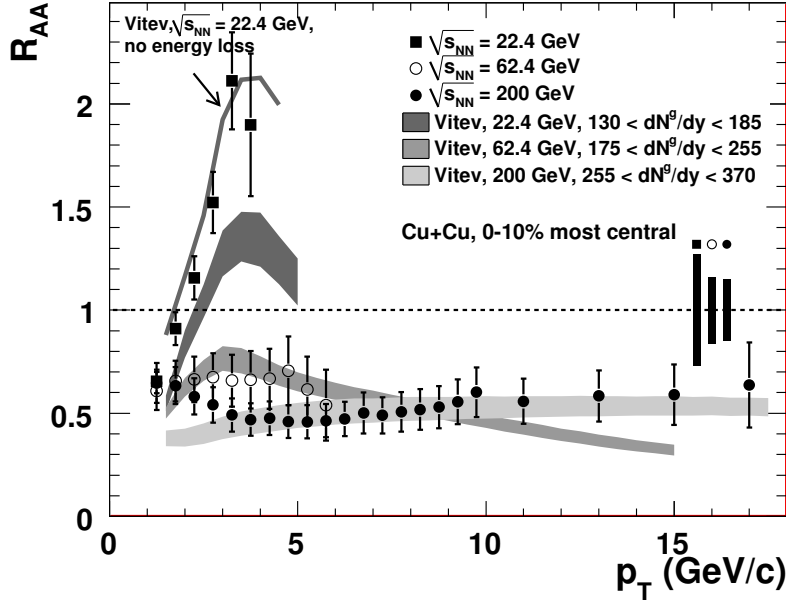


Figure 10: Measured $\pi^0 R_{AA}$ as a function of p_T for the 0 – 10% most central Cu+Cu collisions at $\sqrt{s_{NN}} = 22.4, 62.4, 200$ GeV in comparison to a jet quenching calculation [32]. The error bars represent the quadratic sum of the statistical uncertainties and the point-to-point uncorrelated and correlated systematic uncertainties. The boxes around unity indicate uncertainties related to $\langle N_{\text{coll}} \rangle$ and absolute normalization. The bands for the theory calculation correspond to the assumed range of the initial gluon density dN^g/dy . The thin solid line is a calculation without parton energy loss for central Cu+Cu at $\sqrt{s_{NN}} = 22.4$ GeV.

dileptons from internal conversion of direct photons, similarly to what was done in 200 GeV Au+Au[22]. The dilepton data, particularly with the improved signal/background afforded by the HBD, are also sensitive to the medium modification of hadrons expected from chiral symmetry restoration. It should be noted that the chiral condensate is one of the few, perhaps even the only, known order parameters in the QCD phase transition. Consequently, PHENIX proposes to provide data on this as part of the initial energy scan while the HBD is available.

It is important to measure at the same time the elliptic flow of pions, kaons and protons to see whether v_2 saturation, shown to hold for high \sqrt{s} collisions in Figure 11, sets in at the same point. The magnitude of v_2 , along with its centrality and p_T dependence are the main observables which constrain hydrodynamics calculations (we note that hadron p_T spectra are also important, but they do not pose a significant running time requirement compared to elliptic flow measurements). Comparison of 3-d hydro calculations, especially the trends with centrality and p_T are important to extracting the viscosity to entropy ratio, η/s from the data, utilizing the new approaches, codes, and results being developed

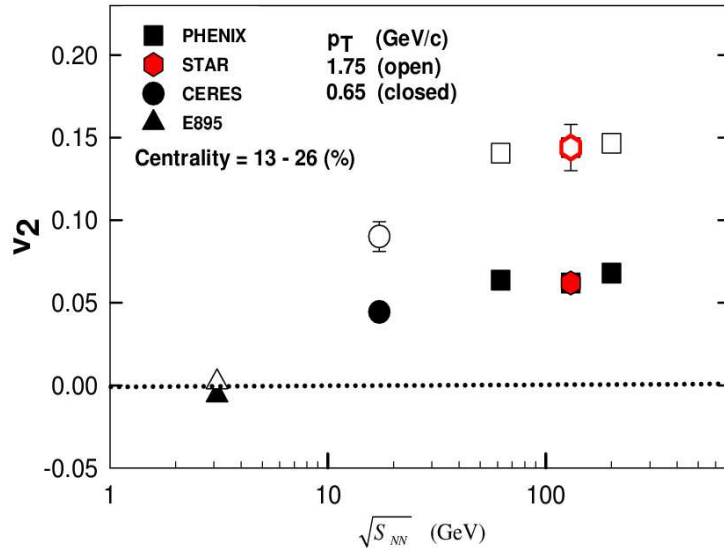


Figure 11: v_2 of charged hadrons at two values of p_T , as a function of $\sqrt{s_{NN}}$ [33]. Results are shown for collision centrality of 13% to 26%.

by theorists in the TECHQM collaboration. Hydrodynamics calculations constrained to reproduce the bulk matter flow are also of key importance to extraction of the initial temperature of the perfect fluid from the observed photon spectrum.[22]

At the deconfinement phase transition, η/s has been predicted to have a minimum value.[34] Such behavior is not only expected at T_c in QCD, but is observed near quantum critical points in other systems such as strongly coupled electromagnetic plasmas[35] and condensed matter systems near a quantum critical point, where near-ideal fluids of electrons are seen[36, 37]. It is natural to ask how the deconfinement phase transition producing minimum η/s at T_c relates to fluid properties at quantum critical endpoints, such as the critical end point predicted to lie between a first and second order phase transition[38]. While they are not in the same place on the phase diagram, it is clear that quantum effects are important at both kinds of critical point in QCD, and the behavior of η/s requires more theoretical work. However, it is very clear that high quality experimental data on bulk flows is needed, along with temperature information to locate it on the phase diagram. Below the critical end point, the quark number scaling of v_2 may be broken, motivating study of baryon and meson flow separately. This goal is a key ingredient in our beam use proposal, as detailed below. Careful comparison to viscous 3-d hydrodynamics calculations will allow extraction of the shear viscosity to entropy ratio, η/s .

Searching for the onset of opacity requires baseline measurement of p+p collisions at the same \sqrt{s} , and ultimately also d+Au collisions to measure the Cronin effect to extract the magnitude of the jet suppression. We propose measurement of p+p collisions

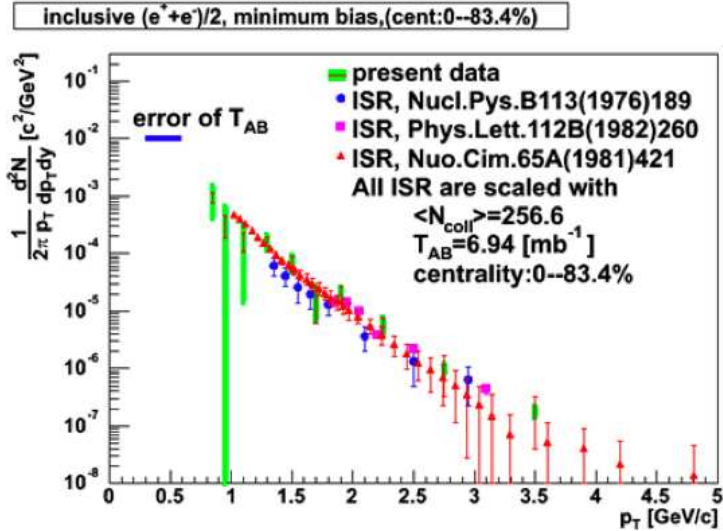


Figure 12: Spectrum of non-photonic electrons in minimum bias Au+Au collisions at 62.4 GeV, compared to p+p collisions at top ISR energy.

at 22.4 GeV in 2010 in order to allow interpolation at energies between 22.4 and 62.4 GeV, using the prescription developed by d’Enterria[39]. We envision a later request for d+Au comparison running.

4.2 Heavy Quark Energy Loss

It is important to determine experimentally whether the opacity to heavy quarks observed in 200 GeV Au+Au collisions sets in at the same point as opacity to light quarks. Answering this question requires measurement of non-photonic electron R_{AA} along with π^0 R_{AA} and v_2 of several additional species of identified hadrons. Preliminary PHENIX results for charm production via semi-leptonic decay to electrons, shown in Figure 12 indicates that at 62.4 GeV, R_{AA} for charm is near 1, contrary to data at higher collision energy and contrary to R_{AA} observed for π^0 . This provides a first hint, albeit with large uncertainty, that the onset of opacity for charm quarks may be at a higher \sqrt{s} than for light quarks. We request sufficient running at 62.4 GeV to determine whether R_{AA} is indeed equal or near to 1.

We have used the energy loss and collective flow of charm quarks to provide constraints

on the viscosity to entropy ratio η/S , independently of comparing light hadron flow to hydrodynamic calculations. The conclusions are limited by the statistical precision of the measurement of single electrons from non-photonic sources. As can be seen in the right panel of Figure 4 above, the improved reaction plane resolution of the RXNP detector and the higher statistics of Run-7 provide a substantial improvement upon the Run-4 result. Nevertheless, a substantially higher statistics obtained by combining Run-7 and Run-10 are crucial to decrease the uncertainties. Beginning in 2011, the VTX detector will provide charm and bottom separation, allowing PHENIX to determine whether bottom quarks also experience significant energy loss and drag in the produced medium; current expectations are for these very heavy quarks to be poorly stopped by the medium. The luminosity increase due to stochastic cooling, along with the new capabilities with vertex detectors, are also key to addressing this question.

4.3 Low Mass Dileptons and Thermal Radiation

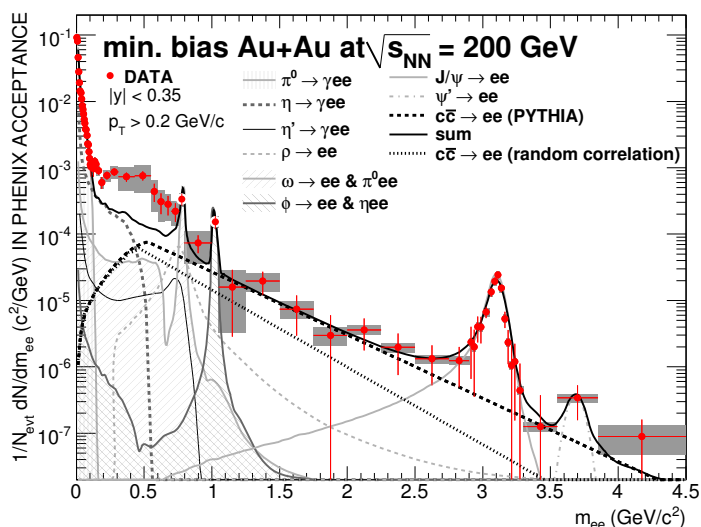


Figure 13: The Run-4 PHENIX minimum bias dielectron yield as a function of invariant mass. Vertical lines represent statistical errors and gray boxes represent systematic errors.

Di-electron measurements in Run-4 Au+Au and Run-5 p+p have shown remarkable features. A large excess is observed at small invariant mass; this is visible as a “bump” above the solid line indicating di-electrons from hadronic sources in Figure 13. No excess is observed in p+p collisions at the same energy. The excess in Au+Au exceeds that in lower energy collisions at CERN, and there is considerable discussion about its source. While the lower energy result is generally interpreted as a medium modification of the ρ meson spectral function, the hadron gas phase of the collision is usually expected to be less dominant at RHIC energy. The centrality and p_T dependence of the excess are under study, but the large combinatorial background causes substantial statistical uncertainties

resulting from the subtraction of two large numbers. The systematic errors are large as well, due to uncertainties in normalization of the combinatorial background. Consequently, the Run-4 data lack the precision required for fine binning in mass, and provide for only limited sensitivity to expected modifications of spectral functions. Rather than a single bin at the ω peak, several-fold finer binning is needed. A four-fold improvement requires a data set with effectively 16 times more statistical and systematic precision. This will also allow us to quantify the centrality and p_T dependence of the excess.

At low mass and high p_T , di-electrons are produced by the same mechanism as direct photons. The p_T spectrum of di-electrons above 1 GeV/ c p_T has a shape characteristic of a sum of pQCD direct photons at high p_T and direct photon “internal” conversions at moderate p_T . PHENIX has submitted a paper analyzing the photons as emission from a thermal source. An initial collision temperature in the range of approximately 300-600 MeV is inferred from the data by comparison to hydrodynamical models which predict photon spectra matching the data. The range in T_{init} arises due to different assumptions about the thermalization time. However, there is a strong correlation between values of T_{init} vs. τ that result in photon spectra that reproduce the observed spectrum. Improved data are crucial both for better precision on T_{init} from better discriminating power among models, and also to determine the centrality dependence of the initial temperature. This measurement must be done in Run-10 while the improved signal to background from the HBD is available.

Successful operation of the HBD offers a unique opportunity for dilepton measurements at energies that have never been studied before. An energy scan between the top RHIC energy and top SPS energy will allow measurement of the dielectron spectrum and also the direct photon spectrum via internal conversions at 62.4 and 39 GeV. As demonstrated below, PHENIX can make completely new measurements in this energy regime. These measurements will help to pin down the evolution of T_{init} as well as hadron medium modification signals in concert with the opacity onset search.

4.4 Color screening and quarkonia

PHENIX has shown that, as predicted, J/ψ are suppressed at RHIC. Surprisingly, the suppression is not extremely different from that observed at the SPS at center of mass energy an order of magnitude lower. New preliminary results from PHENIX indicate that Υ is also suppressed at RHIC, see Figure 14. From the Run-7 data PHENIX has extracted a 90% confidence level upper limit of 0.64 on Υ suppression. While this value may be consistent with what should be expected given contributions of the 2S+3S states, feeddown from χ_b and cold nuclear matter effects, additional data are required for a precision determination of R_{AA} .

A central question about quarkonia suppression is its p_T dependence for J/ψ . There

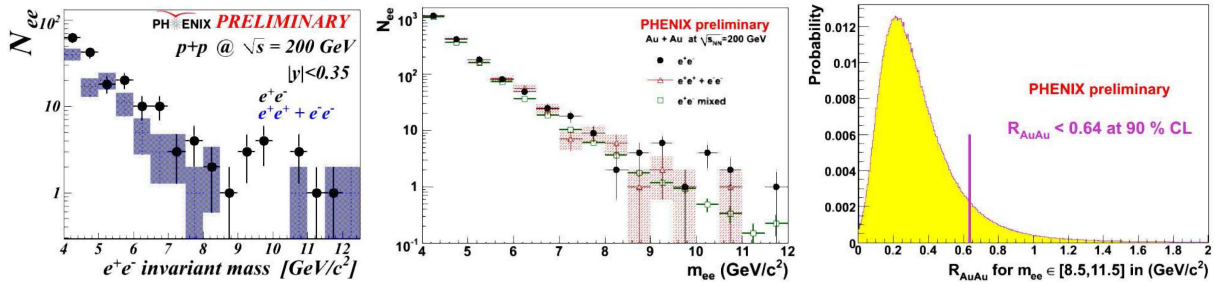


Figure 14: Upsilon production in $p + p$ and suppression in Au+Au collisions.

are several predictions of the high p_T behavior of J/ψ suppression, with different theoretical descriptions predicting opposite trends. Furthermore, there are different conclusions drawn from PHENIX Cu+Cu and p+p data, and a recent STAR analysis using a combination of STAR and PHENIX data for different systems. High quality measurement in Au+Au will sort these out.

J/ψ suppression at forward rapidity is found to exceed that at midrapidity. As these results run counter to expectations from color screening in the medium, there is tremendous theoretical work ongoing to understand them. One possible explanation is that many of the observed J/ψ 's are not in fact primordial, but are regenerated by final state coalescence of charm and anti-charm quarks which have been caught up and scrambled by the medium. This hypothesis can be checked by measuring the elliptic flow of the J/ψ , which requires a very substantial amount of data. An alternative is that, contrary to simple expectations, cold-nuclear matter (CNM) effects are stronger in Au+Au at forward rapidity than at mid rapidity in nucleus-nucleus collisions.

All of these motivate additional high quality, high statistics Au+Au data samples. PHENIX can make definitive measurements addressing the first two questions in Run-10. the J/ψ flow can be determined by combining the requested 200 GeV Au+Au data in Run-10 and Run-11 with the existing, but as yet inconclusive, J/ψ v_2 data from Run-7.

4.5 γ -Jet and Reconstructed Jet Probes

Jets resulting from hard scattered partons traversing the hot, dense partonic medium have proven to be extremely informative probes of the medium. While single hadron suppression and dihadron correlations have been studied extensively already, PHENIX is now pursuing a more ambitious program using rarer processes. In particular we are interested in γ -jet correlations and fully reconstructed jets. Jets correlated with a direct photon have long been considered a “golden channel” for probing the quark gluon plasma. Following the discovery of jet suppression and medium modification, it has become compelling to accept the challenge of reconstructing jets in the high multiplicity environment of heavy

ion collisions.

PHENIX has measured γ_{direct} -jet correlations by unfolding γ_{decay} -h correlations from $\gamma_{inclusive}$ -h. The measurement allows use of QCD Compton scattering to produce energy tagged jets, with rates and distribution calculable in QCD, as probes of the hot, dense medium. Using the photon energy to give the energy of the opposing jet allows a direct measurement of the jet fragmentation function. Figure 1 above shows the resulting fragmentation functions in p+p and central Au+Au collisions. While it is clear to the eye that the presence of the medium produces a steeper fragmentation function, the statistical uncertainties make it difficult to quantify the effect with any precision. It is clearly necessary to collect more data on this channel in both p+p and heavy ion collisions.

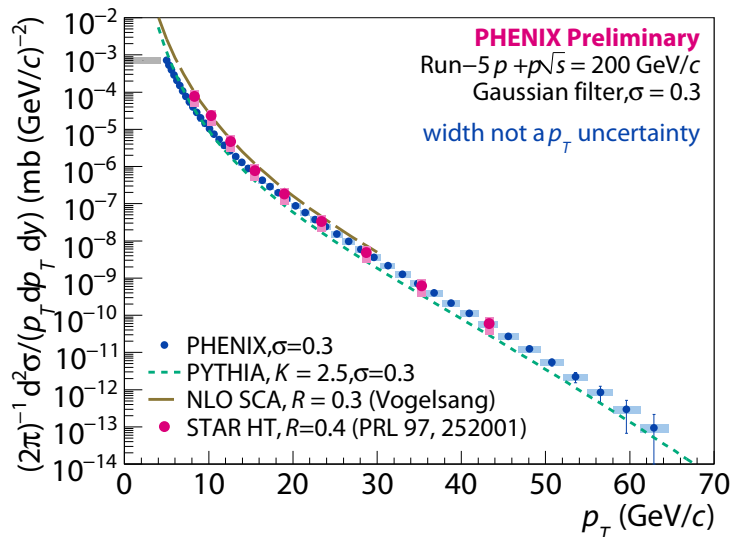


Figure 15: p_T spectrum of reconstructed jets in p+p collisions, compared to several calculations and to measurements by STAR.

Although PHENIX is sometimes referred to as a “limited acceptance” experiment, in fact the acceptance is not small at all. Jets are fully contained in a central arm, allowing use of measured tracks and energy clusters in the EM calorimeter to reconstruct the energy contained in jets. We use a Gaussian filter algorithm, which is seedless and cone-like, but without infrared and collinear unsafety from a hard angular cut-off. The filter shape is chosen to optimize the signal-to-background by focusing on the core of the jet and stabilizing the jet axis in the presence of background. Figure 15 shows the reconstructed jet energy spectrum in p+p collisions. The observed distribution compares well to expectations from pQCD and PYTHIA, as well as to the spectrum measured by STAR. The same algorithm has been applied in Cu+Cu collisions, along with several ways of removing the underlying event background and controlling for event-to-event fluctuations in this background. Figure 16 shows the azimuthal opening angle distribution of reconstructed jet pairs in Cu+Cu. A clear signature of back-to-back jet production is observed, however, the statistical error bars are large.

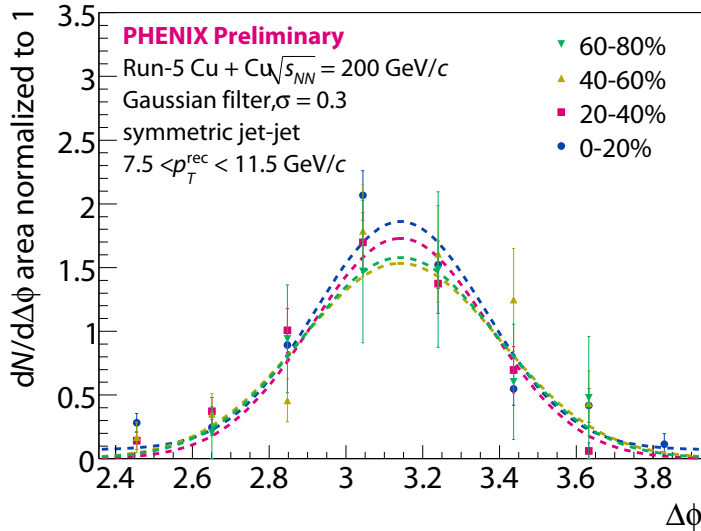


Figure 16: Azimuthal opening angle of reconstructed jets in Cu+Cu collisions at different centralities.

Ultimately we would like to study the reaction plane dependence of photon-tagged and reconstructed jets in order to perform true tomography with these sensitive probes. Of course, this requires considerably larger statistics than have been available to date.

4.6 Search for the QCD Critical End Point

As the results from RHIC indicate that the medium is partonic, rather than hadronic, mapping the QCD phase diagram is key to elucidating the nature of the phase transition. There have been predictions from lattice QCD of the existence of a critical end point, where a first order phase transition between a hadron gas and quark gluon plasma turns into a more subtle “crossover.” This endpoint is predicted to lie at relatively low values of the baryon chemical potential, μ_B , though how low depends on the details of the calculation. There have been several workshops around the world centered upon developing approaches for such a search. Theoretical expectations for the critical point suggest it will be found when the baryon chemical potential is in the range $150 < \mu_B < 500$ MeV. This corresponds to collision energies in the range $5 < \sqrt{s} < 30$ GeV. Rajagopal suggests that it is not necessary to be particularly close to the critical point to be sensitive to it, although other authors disagree. Rajagopal suggests an energy scan in steps of 50-100 MeV in baryochemical potential.

Many signatures have been proposed to help identify the approach to the critical point. We will discuss below the running conditions required to measure these observables. They

Table 2: Relationship between baryon chemical potential and center of mass collision energy.

μ_B	$\sqrt{s_{NN}}$
550	5
470	6.3
410	7.6
380	8.8
300	12.3
220	18
150	28
75	60

vary in complexity and rate, and thus have very different running time requirements.

Femtoscopy provides tools to measure various spatio-temporal dimensions of the hot, dense region. Measurements at top RHIC energy by PHENIX have revealed extended non-gaussian tails in the source function. These tails have been shown to be sensitive to emission time. Increased emission times, as expected for a first order phase transition, may result in an increased tail in the 1-D source functions. In addition, a second order phase transition may also be reflected in non-gaussian Levy like shapes of the source function.

The observation of critical opalescence would be a clear signature of a QCD Critical Point. Optical opacity is a function of nuclear modification factor and the distance covered by the attenuated jet in the medium. An excitation function of R_{AA} may allow for a determination of the maximum of opacity as a function of colliding energy and centrality. Azimuthally sensitive HBT measurements allow directionally dependent studies of spatial dimensions, that add valuable information to directional dependent R_{AA} measurements. Clearly, the search for such a signal is limited to collision energies where the cross sections of jet probes are large enough to produce the probes at a measurable rate. Furthermore, the data sample must be large enough to allow measurement of reaction plane dependence of both R_{AA} and HBT.

A number of predicted critical point signatures involve non-statistical fluctuations in quantities such as event multiplicity, mean transverse momentum, K/π ratio, and multiplicity fluctuations in the longitudinal direction. While such fluctuations are expected as one approaches the critical point, a number have been investigated at the SPS and found to be featureless as a function of \sqrt{s} . However longitudinal correlations remain of interest as PHENIX has observed a feature in semi-peripheral Au+Au collisions at full energy[24]. Density fluctuations at the critical point may make it difficult to transport momentum over large distances, thereby decreasing η/s . Sensitivity to this, however,

requires more than simply measuring the presence of fluctuations. The strength of the fluctuations must be determined, with sufficient theoretical guidance in hand to translate the observable into a measure of the correlation length. Other systems near quantum critical points exhibit fluctuations over temperature and density scales that vary greatly. Arrival at the critical point is signaled by the onset of extremely long-range correlations. Critical exponents persist well past the density corresponding the quantum critical point in such systems. Further development of approaches at RHIC, particularly given the small system size, short life, and time integral nature of the observables, will be important for the success of a credible critical endpoint search.

Identified particle spectra are useful tools to characterize the hadron gas phase of the collision. The measurement of identified particle ratios, including K/π and proton-to-antiproton ratios are necessary to measure the location of the system on the QCD phase diagram. In addition, the measurement of proton-to-antiproton ratios may serve as an additional signal for the presence of the critical point if the QCD critical point serves as an attractor of hydrodynamic trajectories in the $\mu_b - T$ plane describing the expansion of the hot matter. With the addition of a new start-time detector with acceptance optimized for low energy energy collisions, measurements of identified particle ratios will be accessible to PHENIX at collision energies below 17 GeV. From the hadron ratios and spectra, the freeze-out temperature and radial flow of the hadrons, which reflect the expansion velocity can be extracted.

4.7 Projected Physics Performance

4.7.1 Low Mass dileptons with HBD in Run-10

The effectiveness of the HBD in distinguishing closely separated electron pairs from isolated single electrons has been demonstrated in initial analysis of the Run-9 p+p data. 20 photo-electron are observed in the HBD for each electron traversing it.

Figure 13 shows that the existing results for low mass dielectrons are limited by systematic uncertainties[40]. These are dominated by the uncertainty in normalizing the large combinatorial background. The HBD will reduce this combinatorial background, thereby reducing both the systematic and statistical errors. To quantify the expected effect, we define an effective signal size, S_{eff} as the number of signal counts in a background-free measurement that would have the same relative error bar as our final measurement. We use this quantity in order to put together the various effects of the HBD. While rejection of double electrons in the HBD improves the background, placement of the single-double cut also affects the efficiency of tagging single electrons (the signal). Furthermore, the HBD introduces material into the PHENIX acceptance and so produces an additional background. S_{eff} quantifies these competing effects, and allows comparison of the ex-

pected performance to that observed in PHENIX in Run-4 with no HBD. The expression below shows how this effective signal size depends upon the signal and background terms:

$$\frac{1}{\sqrt{S_{eff}}} = \frac{\sqrt{\sigma_{stat}^1 + \sigma_{sys}^2}}{S} = \frac{\sqrt{(\sqrt{S + BG})^2 + (BG \times \sqrt{\sigma_{LikeSign}^2 + (0.2\%)^2})^2}}{S}$$

Simulated signal and background were generated using an electron cocktail tuned to PHENIX measurements. The HBD performance was simulated for two extreme cases: (i) accounting only for HBD-based single- double separation, (ii) accounting for both single-double separation and increased purity of the electron sample due to additional electron-ID from the HBD. Analysis of Run-7 and Run-9 data indicate that the actual HBD performance lies between these two extremes.

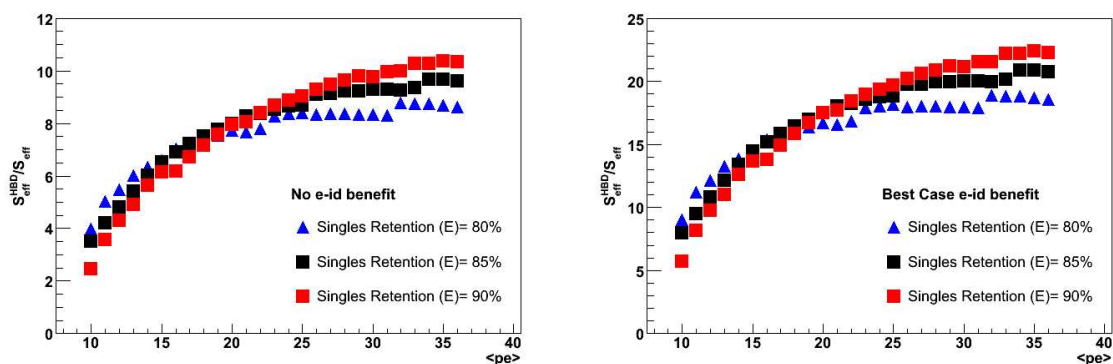


Figure 17: The ratio of the effective signal with the HBD over that without an HBD is shown as a function of the raw photo- electron yield. The left panel assumes no benefit from additional electron- ID using the HBD. The right panel assumes the theoretical maximum additional electron ID in the HBD. The different symbols show performance with different cuts to separate single from double electrons; the cut effect is quantified via the single electron signal retention performance. The HBD in Run-9 yields 20 photo-electrons and electron identification performance in between these two extremes.

Figure 17 shows the ratio of effective signal with an HBD to that of baseline PHENIX without the HBD, as a function of the number of photoelectrons detected by the HBD. The effective signal is calculated without (left panel) and with (right panel) accounting for HBD eID performance. The range of the plot extends from below the Run-7 result (14 photo-electrons) to the ideal performance (36 photo-electrons). The three curves on each side correspond to different cut values separating single from double electrons. They cross one another because S_{eff} depends both on the signal level, S , and, with a different functional form, on the background level, BG . With the observed HBD response of 20

photo-electrons, we expect an improvement in effective S/B by at least a factor of 8, and more likely nearer to 16.

Figure 18 shows the ratio of the effective statistics of dielectrons in the low mass region as a function of the length of AuAu running time, f . Here f is the ratio of Run-10 integrated luminosity to that of Run-4. For a physics run collecting integrated luminosity comparable to that of Run-7 (i.e. 0.8 nb^{-1} recorded), the effective statistics of the low mass dielectron measurement would be increased by a factor of 22 over the existing Run-4 result. This estimate assumes no improvement in photoelectron performance and no benefit from electron ID in the HBD; with anticipated performance improvements the effective statistics ratio is likely to increase over Run-4 by a factor closer to 52. Thus, a Au+Au run approximately equivalent to Run-7 with the HBD in place would reduce the overall error of the dielectron measurements by a factor of approximately 7. Our requested integrated luminosity is closer to twice that collected in Run-7, so the improvement will be better. This will allow study of the mass, p_T , and centrality of the large low mass excess observed by PHENIX. Collecting this data set in Run-10 will achieve the dielectron measurement for which the HBD was built.

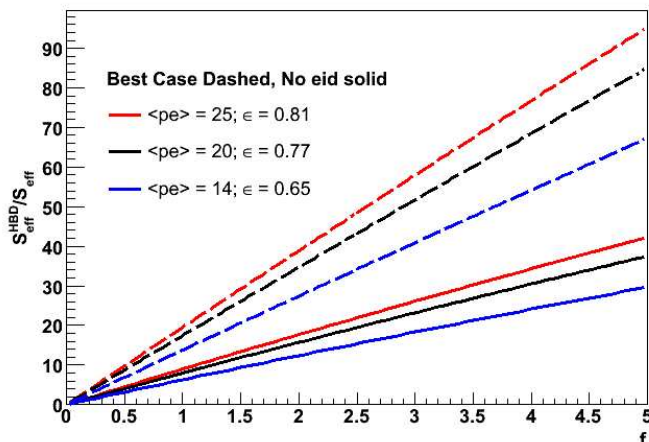


Figure 18: The effective signal relative to that in Run-4 is plotted as a function of the ratio of Run-10 integrated luminosity divided by Run-4 integrated luminosity. Note that the HBD response measured in Run-9 is 20 photoelectrons.

Figure 19 shows the NA60 measurement of the spectral function of the ρ meson in central In+In collisions at $\sqrt{s} = 17 \text{ GeV}$ per nucleon pair[41]; $25 \text{ MeV}/c^2$ mass bins allow determination of the shape of the distribution. These data have been used to challenge many of the models of ρ in-medium broadening at the density and temperature achieved in full energy collisions at the SPS. It is imperative to constrain those explanations by comparison to broadening and possible mass shifts in the much hotter, initially partonic, medium at RHIC. This measurement is an essential ingredient to separating effects of the hot hadron gas from partonic effects at RHIC. Comparison of this plot to Figure 9 shows

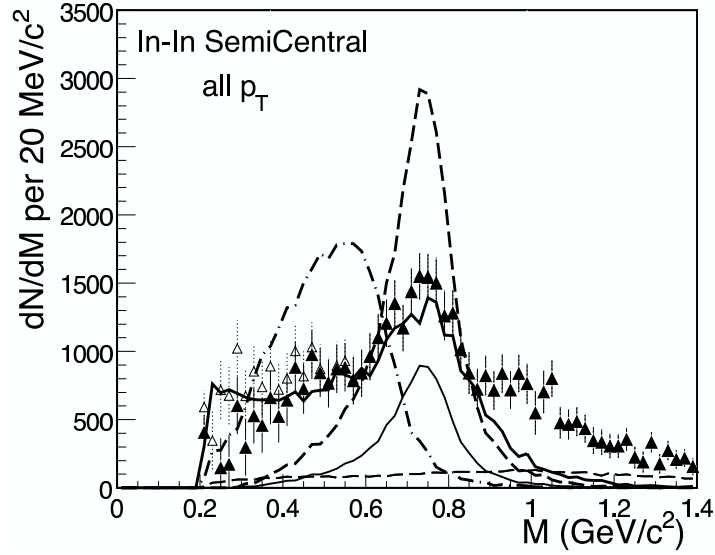


Figure 19: ρ spectral function measurement at by NA60 at $\sqrt{s} = 17$ GeV[41] compared to several theoretical models. Note the mass bin size of $25 \text{ MeV}/c^2$.

that such an analysis would be impossible in PHENIX without the background rejection from the HBD. However, with a factor of approximately 8 improvement in total error, the PHENIX measurement of the spectral function would have similar error bars to those of NA60 in similarly fine bins.

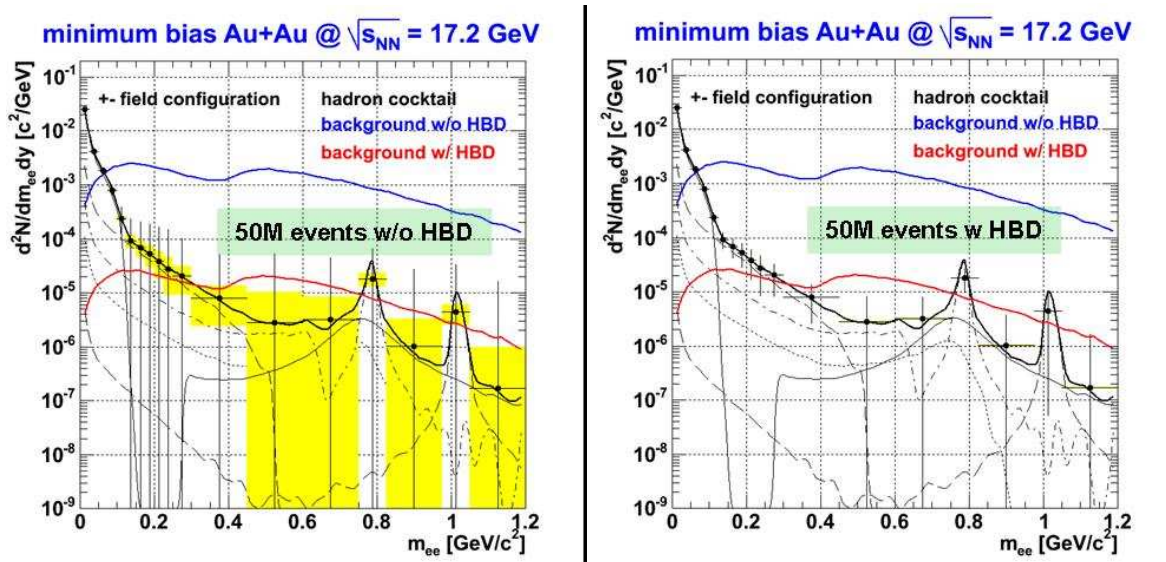


Figure 20: Simulated low-mass dielectron cocktails (signal and combinatorial background) for 50 million Au+Au collisions at 17.2 GeV (left) without the HBD and (right) with the HBD installed in PHENIX. The boxes in the left plot indicate the systematic uncertainty.

Running at 62.4 and 39 GeV in Run-10 with the proposed integrated luminosities will allow dielectron measurements in a region that has never been studied before. The low mass dilepton excess observed by PHENIX seems to have different characteristics from the one observed at the SPS. It is not reproduced by the models that describe the SPS results. These two facts could indicate that a different source is at the origin of the excess at the top RHIC energy and therefore a study of the dilepton spectrum from top SPS energy to top RHIC energy will be very interesting to study the onset of this new source. The size of the required event sample varies strongly with \sqrt{s} , as the combinatorial background scales as the square of the multiplicity. Figure 20 is the result of a simulation of the dielectron spectrum in 50 million Au+Au events at 17.2 GeV. Comparing the right and left panels illustrates that without the HBD, many more than 50 million events are required for a measurement of the dielectron spectrum, owing to the large background. With the improvement in S/B afforded by the HBD, the error bars decrease substantially. Even so, 50 million events are an absolute minimum sample for a “first look” type measurement. Unfortunately, the collisions rates predicted at this energy are so low as to preclude collection of a data set of this magnitude at 17 GeV. However, given the knowledge from the SPS, it is the intermediate energies which are of interest. Fortunately, the collision rates increase as E^2 , so it is possible to 350 million events at 62.4 GeV and 50 million at 39 GeV.

4.7.2 Heavy Flavor in Run-10

One of the exciting results from Run-7 is the first observation of Υ suppression in heavy ion collisions. However, the result has sufficiently poor statistics that only an upper limit on R_{AA} can be made. One of the major goals in the near future is to improve this measurement and understand whether the observed Υ suppression is from feeddown and cold nuclear matter absorption, or whether the hot, dense partonic matter also suppresses Υ s. Under the assumption that we will collect twice the Run-7 Au+Au data set in Run-10, and three times the Run-6 p+p reference sample in the ongoing Run-9 (combining it with Run-6, if needed), R_{AA} can be measured with a 10% statistical uncertainty. This estimate uses the most probable value from Run-7. Figure 21 shows the narrowing of the R_{AA} probability distribution expected from the Run-10 data; this will allow assigning a value for R_{AA} .

Run-10 will allow a substantial improvement in the measurement of open heavy flavor flow. Figure 22 indicates the expected uncertainties. The measurement will finally reach the quality required for good discriminating power among models of heavy quark energy loss.

We will search for evidence of heavy quark recombination to produce J/ψ at freeze-out, which would mask suppression by the color screening early in the collision. This is accomplished by measuring the J/ψ elliptic flow. This requires a substantially larger

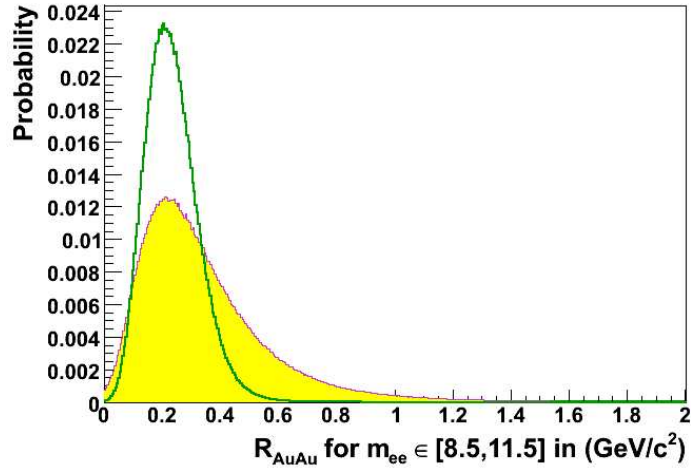


Figure 21: The probability for R_{AA} of Υ from Run-7 Au+Au which yields a 90% C.L. upper limit of 0.64 (yellow), and a projection of the accuracy obtained by addition of Run-10 with twice the integrated luminosity (green).

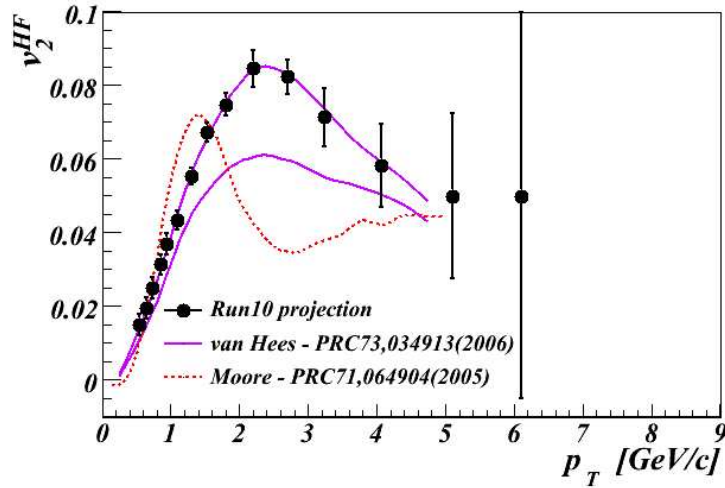


Figure 22: Projected probability distribution for Υ in Run-10, green, compared to that measured in Run-7 (yellow).

Au+Au data set than was taken in Run-7. Figure 23 shows a preliminary result from approximately half of the Run-7 data on $J/\psi \rightarrow e^+e^-$. Clearly the data as yet lack the required statistical precision. Figure 24 shows the quality of the measurement expected from a data set twice that of Run-7; the resulting measurement will not have small enough errors to definitively prove or rule out J/ψ flow. this will be achieved by combining the Run-7 result, with those of the planned Run-10 and Run-11 Au+Au samples.

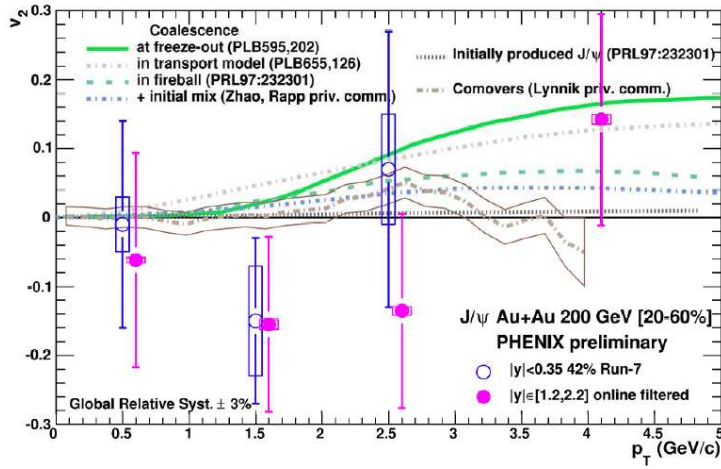


Figure 23: Preliminary analysis of Run-7 data on flow of J/ψ detected in the e^+e^- and $\mu^+\mu^-$ channels. The plot contains approximately half of the data.

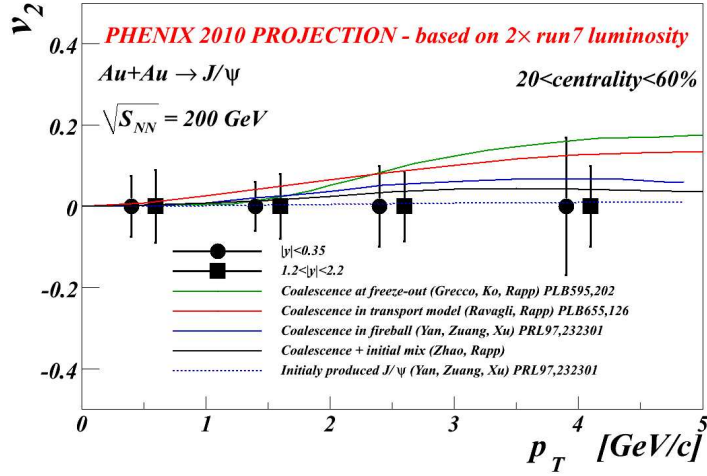


Figure 24: Projected sensitivity to J/ψ v_2 in Run-7 + Run-10 data sets combined.

4.7.3 Jet Probes in Run-10

As shown above, PHENIX has made first measurements in the γ -jet channel in Run-4 and Run-7. It is clear that the statistical uncertainties from those runs remain prohibitively large. However, the proposed Au+Au running in Run-10, when combined with the existing Run-7 results, will provide discriminating power between different mechanisms for medium-induced energy loss. Figure 25 shows the projected performance for this measurement. We measure the conditional yield (per-trigger yield) of hadrons as a function of p_T , associated on the away side of direct photon triggers in both p+p and in central Au+Au collisions. The figure shows the ratio of Au+Au to p+p yields, I_{AA} , for different

energy direct photon triggers in the four panels. The ratios are plotted as function of $z_T = p_T^{\text{hadron}}/p_T^\gamma$. For direct photon triggers, this is a plot of the medium modification of the jet fragmentation function. The three different curves are from three different theoretical calculations incorporating different treatments of the energy loss mechanism. The blue band, which has the weakest dependence upon z_T , show a calculation from Renk[42] which follows the in-medium shower evolution, averaging over the hydrodynamic expansion of the medium. The triplet of thin black curves show the results of a NLO pQCD calculation of the medium-induced energy loss[43]; the radiated gluons induced by the medium add low z_T particles in the jet cone, and so retain a correlation with the trigger photon direction. The solid black line shows a calculation using a Modified Leading Logarithm algorithm[44], which enhances the gluon splitting and produces a larger number of soft hadrons.

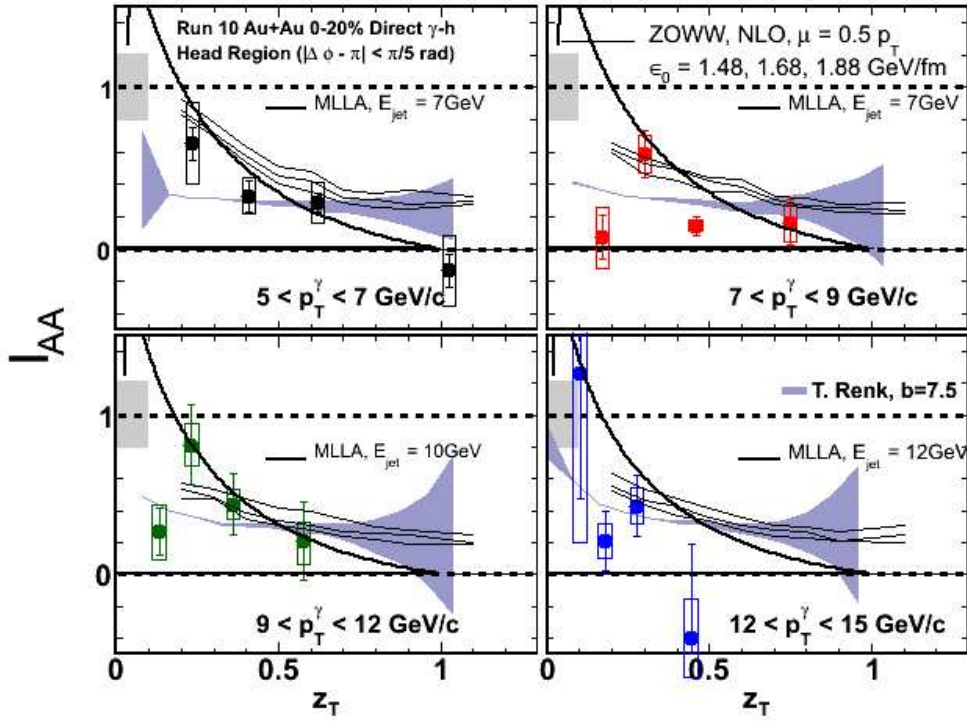


Figure 25: Projected I_{AA} sensitivity in Run-10. Data are Run-7 points, with error bars scaled for Run-7+Run-10 statistics. See text for description of theoretical curves.

While the Run-7 statistics are insufficient to determine which set of assumptions about the medium effect are correct, the data to be collected in Run-10 will distinguish among the available models.

4.7.4 Search for perfect liquid onset between 22 and 62.4 GeV

For PHENIX, measuring the excitation function of R_{AA} is of paramount importance in an energy scan. The exact conditions (energy, system size) where parton energy loss sets in will have major constraining power on theory - the more so because these conditions should be different for light and heavy quarks. Although an R_{AA} measurement up to the minimum acceptable p_T requires high statistics, the relevant energy range is mostly above RHIC injection energy, where the rates collision rates remain reasonable. The requirement of significant statistics is particularly relevant for electrons from heavy-quark decays, where 62.4 and 100 GeV have been identified as the most promising energies. The measurements will require p+p reference data. In addition, d+Au data at the same energy points would be highly desirable to constrain cold nuclear matter effects. We note that while R_{AA} is probably not sensitive to the critical endpoint *per se*, if “critical opalescence” exists it is one of the key observables of a critical endpoint. Accordingly, our expectation is a relatively smooth excitation function, and we base our estimates of required statistics accordingly and require less than 10 or 15% statistical error. Should critical opalescence indeed appear, it would cause an anomaly in the excitation function (energy loss suddenly becoming very large at the critical point) which would be easy to see even with lower statistics or at lower energies.

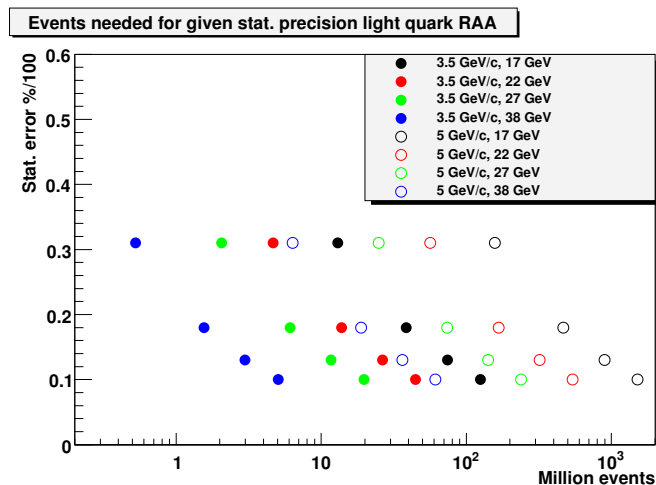


Figure 26: Events necessary to measure 0 RAA with given statistical error up to 3.5 and 5 GeV/c transverse momenta

Figure 26 illustrates the dependence of the statistical error on R_{AA} at 3.5 and 5 GeV/c p_T in Au+Au collisions at different energies. What is plotted is the statistical error on π^0 vs. the number of events in collisions at $\sqrt{s} = 17, 22, 27$ and 39 GeV. Note that the systematic error is expected to be about 10%, therefore, decreasing statistical error below 10% provides no real improvement on the measurement.

The measurement of heavy-quark energy loss will provides crucial information in addi-

tion to the light-meson R_{AA} measurements. The large mass of the charm quark introduces a new scale. PHENIX discovered that the R_{AA} of electrons from heavy-flavor decays indicates similar energy loss to light quark or gluon jets. Since this cannot be explained via induced gluon radiation alone, such measurements provide crucial information to pin down the energy loss mechanism(s).

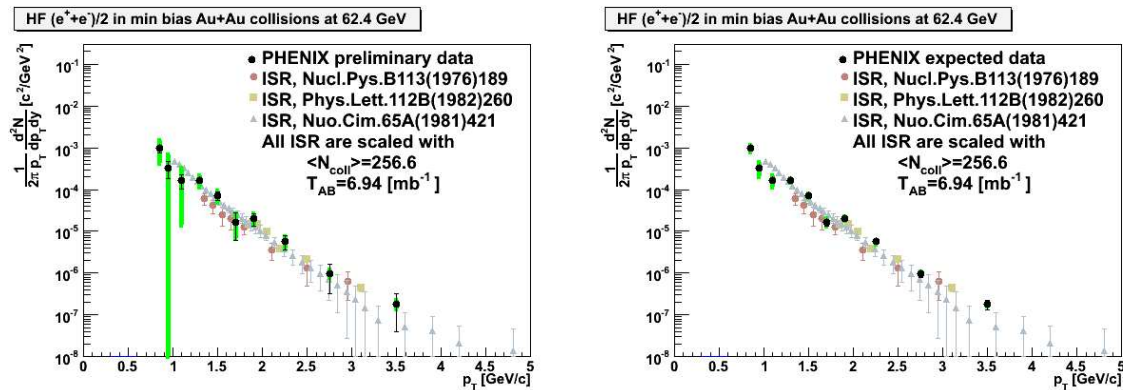


Figure 27: Left: Single non-photonic electron spectrum measured by PHENIX in 62.4 GeV Au+Au collisions. The comparison points are from several different measurements at the ISR. Right: Projected spectrum from Run-10.

Preliminary PHENIX results for non-photonic electrons, shown in the left panel of Figure 27 suggest that at 62.4 GeV R_{AA} for charm is consistent with unity, indicating an onset of opacity to charm quarks at a *different* \sqrt{s} than to light quarks and gluons. The preliminary PHENIX result at 62.4 GeV is not conclusive due to statistical limitations of less than 30 million minimum bias Au+Au events. Reaching $p_T \approx 5$ GeV/c requires about a factor of ten more statistics, i.e. about 300 million events without and about 50 million events with the photon converter installed at 62.4 GeV. This is the driver for our running time request at 62.4 GeV. The expected spectrum is shown in the right panel of Figure 27. Under the assumption that the uncertainties in R_{AA} are dominated by the Au+Au data, the projected error bars on R_{AA} are plotted in Figure 28. It should be noted that the signal-to-background ratio in the existing 62.4 GeV data is ≈ 0.2 at $p_T = 1$ GeV/c, growing to ≈ 0.5 for p_T above 2 GeV/c). These values are improved significantly by the HBD.

R_{AA} measurements up to at least $p_T = 5$ GeV/c for both pions and electrons are required in order to study jet fragments, rather than particles emitted from the collectively flowing bulk of the medium. For the pions, the event requirement was obtained by requiring 30 counts in the 4-5 GeV/c p_T bin for 0-10% collisions.

Measurements of R_{AA} require p+p collision data at the same energy for the denominator. While the parameterization from d'Enterria[39] can be used in the short run to interpolate, it is important to pin the parameterization to measured data at both high and low energy. We note that existing data on ion collisions at 22.4 GeV lack comparison

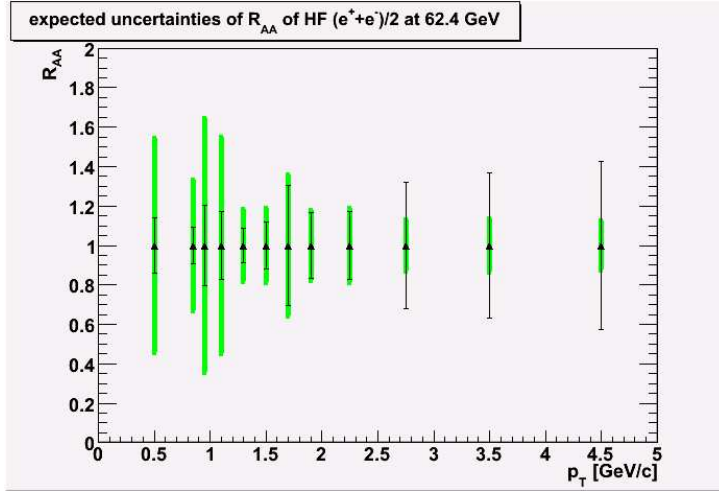


Figure 28: Projected statistical and systematic uncertainties on non-photonic electron R_{AA} in 62.4 GeV Au+Au.

p+p data from RHIC; the observed onset makes it compelling to make this measurement and remove uncertainties inherent in using data from the ISR as the denominator in R_{AA} . Though PHENIX has p+p data at 62.4 GeV, it is insufficient to provide the baseline measurement for non-photonic electrons. We anticipate requesting such a run in the near future. We note that the running times for the higher energy data sets are quite short, and believe that a half week period should suffice for changeover time and data collection.

4.7.5 Search for critical point at lower energies

In the search for the QCD critical point it would be ideal to collect substantial data sets at most of the collision energies listed in Table 2. 100 M events at each energy would allow measurement of di-electrons and di-hadron correlations. Given the baseline luminosity *and collision vertex length* projections, such data sets are only feasible above transition energy (and above SPS top energy). A potential approach could be to collect a substantial dataset for one collision energy that overlaps with the SPS. However, even at the highest SPS energy this would consume a prohibitively large fraction of one year's running time.

The impact of limited data set size can be seen from Table 3, which shows the number of events required for different critical point signatures. Below RHIC transition energy, the storage RF cannot be used, causing the beam to fill the time buckets and blow up in the transverse direction. This dramatically reduces the luminosity. Consequently, multiple datasets of only a few million events are realistically possible. With such datasets PHENIX can measure $\langle N_{ch} \rangle$ and $\langle p_T \rangle$ fluctuations and identified particle spectra with limited centrality selection. Though these would allow a search for non-statistical fluctu-

Table 3: Million Au+Au events required for significant measurement of different observables at various collision energies. The HBT and imaging related observables were evaluated for 10% relative statistical error.

$\sqrt{s_{NN}}$	Fluctuations in $\langle n \rangle$	Fluctuations in $\langle p_t \rangle$	PID spectra, identified particle ratios	longitudinal density correlations critical exponent η	1D imaging of pion source Lévy exponent α 3d Gaussian HBT radii for pions $R_i(m_T)$ HBT intercept parameter $\lambda(m_T)$	dielectron spectra fluctuations if $\langle K/\pi \rangle$	dihadron correlations nuclear modification factor R_{AA} optical opacity κ	heavy flavour electrons 1d image of kaon source 3d image of pion source Kaon 3d Gaussian HBT radii $R_i(m_T)$
5.5	0.01	0.03	0.03	2	54	50	375 NA	NA 953
7.7	0.01	0.03	0.02	2	33	50	246 NA	NA 586
11.5	0.01	0.03	0.02	2	24	50	160 NA	NA 431
17.3	0.01	0.03	0.01	2	19	50	109 157	NA 340
27	0.01	0.03	0.01	2	16	50	68 24	NA 276
39	0.01	0.03	0.01	2	14	50	48 6.3	700 239

ations in particle production and analysis with thermal models of hadron gas freezeout, it is unclear how competitive such data sets would be with those already produced by SPS experiments. Furthermore, operating RHIC experiments in a regime that does not provide for a wide variety of observables to characterize the system, and lacking robust comparison p+p and d+Au data, would represent a major deviation from the approach to discovery science that has proven so successful at RHIC.

Also included in Table 3 are the numbers of event required for PHENIX measurements of other predicted signals of the QCD critical endpoint. Measurements of *susceptibility* \times *temperature*, which is relevant to a 2nd order phase transition are possible from differential analysis of multiplicity fluctuations in the longitudinal direction. Given the multiplicity per event in one PHENIX arm, this can be measured in Au+Au collisions down to $\sqrt{s_{NN}} = 10$ GeV. Two million events are necessary for analysis with 5lower p_T threshold, the magnetic field off condition is best. Given the minimum statistics and the field off requirement while other analyses require the field on, data taking for this observable is best performed in Au+Au collisions above $\sqrt{s_{NN}} = 39.0$ GeV where it can

be done in a few days. Once the silicon vertex detectors are installed, this measurement benefits from the much larger acceptance and is expandable to lower energies.

Femtoscopia provides a number of experimental control tools to measure various spatio-temporal dimensions of the fireballs created in high energy heavy ion collisions. Non-gaussian tails in the source function are sensitive to emission time effects. Increased emission times as expected for a first order phase transition, may result in an increased tail in the 1-D source functions. Consequently, it is of great interest to perform an excitation function with sufficient statistics to explore such tails in the source function. We have estimated the required number of events from our analysis of data at 200 GeV, scaled by the charged particle multiplicity. In addition, a second order phase transition may be reflected in non-gaussian Levy like shapes of the source function. Based on the rate estimates from CA-D and the required event samples given in Table 3, these observables may be accessed above injection energy.

At energies above injection, but below full energy, RHIC is poised to make a unique and substantial contribution to the low baryon chemical potential end of the critical point search. This requires similar conditions to quantification of the onset of light-quark and heavy-quark opacities. With 10 weeks of running, substantial datasets (between 50 and 300 M events) can be collected at several different, allowing analyses of many possible signatures. Given the current uncertainty about which observables will prove most informative, it is imperative to measure as many as possible simultaneously. Consequently, we propose an energy scan of several steps above injection energy is the right first step toward locating the QCD critical point at RHIC.

Below RHIC transition energy, the collision rates become extremely low. Furthermore, the multiplicity falls dramatically, so the triggers designed for full energy RHIC running become very inefficient. In Run-10, PHENIX can trigger effectively using the RXNP detector, which also provides the start time for time-of-flight measurements. After Run-10, the RXNP detector will be removed as it is incompatible with the VTX and FVTX. For the very low multiplicities produced at low \sqrt{s} , the large acceptance of the VTX is extremely advantageous. In particular, the vertex detector will offer improved centrality determination and multiplicity fluctuation measurements. Though it may be possible to trigger using the VTX, a start time signal is necessary and cannot be derived from VTX information. Consequently, PHENIX will design and fabricate a start time/trigger barrel to be located outside the VTX. We request that sub-injection energy running be scheduled after the VTX and new barrel are ready. Furthermore, as the enhanced luminosity afforded by electron cooling in the AGS would make the sub-injection energy running much more efficient, we propose doing the lower energy part of the scan after this capability is available.

5 Discoveries and Future Goals of the Spin Program

5.1 Overview

The highest priority for PHENIX Spin for Runs 10-14 is the completion of the 500 GeV longitudinal spin program described in [13]. This plan requires recording 300 pb⁻¹ at PHENIX, which implies the delivery of approximately 900 pb⁻¹ to our interaction point. These data will enable us not only to make significant measurements of the gluon spin polarization in the proton, using a variety of probes, but also to measure single-spin asymmetries in W production leading to the measurement of the light-quark and -antiquark spin polarizations.

At the end of Run-9, PHENIX will have recorded a total of approximately 25-30 pb⁻¹ (summed over Runs 5, 6, and 9) of polarized pp collisions at 200 GeV. Our goal at 200 GeV had been to record approximately 70 pb⁻¹, however it has become clear that at the current rate of luminosity delivery it will take several more years to achieve this goal. Our analysis of 9 pb⁻¹ of that data (summed over Runs 5 and 6) shows that the double spin asymmetry in inclusive π^0 production, $A_{LL}^{\pi^0}$, is consistent with zero in the transverse momentum range $1 < p_T < 10$ GeV/ c , limiting the gluon spin contribution to the proton spin in the parton momentum range $0.02 < x_g < 0.3$ to $-0.7 < \Delta G^{[0.02,0.3]} < 0.5$ at 3σ [arXiv:0810.0694, accepted for publication in PRL]. As was shown in our Beam Use Proposal in 2008, the additional data we are collecting in Run-9 will provide significant additional constraints on $\Delta G^{[0.02,0.3]}$. We foresee the necessity to move forward and begin the accumulation of statistics at 500 GeV, so that we can extend our range of exploration of gluon polarization to smaller x_g , and begin to explore the spin polarization of u , d , \bar{u} , and \bar{d} quarks via the parity-violating asymmetry in W^+ and W^- production.

Measurement of the direct photon asymmetry will give an independent determination of ΔG . In direct photon production the gluon Compton process ($qg \rightarrow q\gamma$) is dominant, so the double helicity asymmetry will be linear with gluon polarization. Consequently, PHENIX will be able to measure both the sign and value of ΔG through this channel. The expected sensitivities for direct photon A_{LL} from Run9 will, however, still be below the level required to constrain ΔG ; an additional factor of 2-3 is required, given that our Run6 π^0 data already indicate that ΔG is not large in the probed x-range. The higher luminosity of collisions at 500 GeV will put this probe within reach.

In Run-9 there was a very successful engineering run for polarized proton collisions at 500 GeV, in which a tremendous amount of progress was made by CAD. The first series of 500 GeV stores were provided to the experiments, which will provide both important cross section measurements as well as initial results on backgrounds at 500 GeV. Some problems were found during this engineering run which remain to be resolved, the most significant of which was the polarization loss in RHIC in the ramp between 100 and 250 GeV. Even

so the polarization in RHIC was approximately 35-40%. Some additional APEX studies are planned during Run-9 to study the 250 GeV ramp further. It is imperative that at least 60% polarization be achieved at 500 GeV in order to make the spin physics program at this energy feasible.

Based on these considerations, PHENIX proposes the following general schedule for luminosity delivery at 500 GeV during the next few years. The goal is to reach approximately 900 pb⁻¹ delivered to the experiments by the end of 2014, roughly consistent with the delivery rates outlined in the RHIC Spin Plan document but taking into account some lessons learned from the 500 GeV engineering run.

Run-10: 500 GeV machine development (to achieve 60% polarization and optimize luminosity delivery)

Run-11: 150 pb⁻¹ delivered to experiments

Run-12: 230 pb⁻¹ delivered to experiments

Run-13: 250 pb⁻¹ delivered to experiments

Run-14: 270 pb⁻¹ delivered to experiments

It is imperative to collect sufficient data before 2013 to achieve NSAC milestone HP8, which requires measurement of flavor-identified q and \bar{q} contributions to the spin of the proton via the longitudinal-spin asymmetry of W production in calendar year 2013. While this milestone can probably be at least partially satisfied with a subset of 900 pb⁻¹ delivered luminosity, a sufficient amount of data for a first result must be collected in time.

In Runs 11-14, the beam polarizations should be at least 60%. The exact number of weeks and timing of the 500 GeV periods would be determined on a year-by-year basis, depending on the proven performance in each previous year and available running time for RHIC.

One may wonder – why start with 150 pb⁻¹ in Run-11? The mean projection from CAD for Run-9 for 10 weeks of 500 GeV running is 200 pb⁻¹ delivered to the experiments. Our request is based on the luminosity delivery during the engineering run. To obtain this number, we looked at the average over all fills in the last three weeks of the engineering run and asked “What if we got 10 fills like that every week for 10 weeks?” The answer was a delivered luminosity of 125 pb⁻¹. We should safely expect that much and in fact somewhat more if machine development is permitted in Run-10. On this basis we set a goal of 150 pb⁻¹ delivered in Run-11, and we expect that CAD will be able to achieve that and make additional improvements in subsequent runs. The delivery targets we show for Runs 12-14 are consistent with the RHIC Spin Plan document (but shifted by one year).

PHENIX can make good use of substantial 500 GeV running already in Run-11. While it is true that not all of our upgrades for spin physics will be installed, we will already be in a position to begin the 500 GeV program in earnest. Our central arms are ready to begin the program now. In the muon arms, installation of the muTrigger upgrade electronics (which is partially complete already) and the large RPC3 detectors planned for Run-11 will provide essentially the full rejection power at the trigger level. The RPC1s, which will be installed in the following year, will provide additional timing and pointing information. This added rejection power is especially useful to improve our ability to reject cosmic backgrounds in *offline* analysis. However, the timing from the RPC3 chambers will already provide a significant cosmic background rejection power.

5.2 Expectation for Light-Quark and -Antiquark Spin Polarization Measurements

The parity-violating asymmetry $A_L^{W^\pm}$ in the production of W^\pm bosons permits the determination of the light-quark and -antiquark polarizations in the proton. In PHENIX this will be done via the detection of high p_T electrons/positrons in the central arms from the decay $W^\pm \rightarrow e^\pm \nu$ and of high p_T muons in the muon arms from $W^\pm \rightarrow \mu^\pm \nu$. Our simultaneous coverage in forward, backward, and central rapidity will provide a powerful means of determining the quantities $\Delta u/u$, $\Delta d/d$, $\Delta \bar{u}/\bar{u}$, and $\Delta \bar{d}/\bar{d}$ in the parton momentum range $0.05 < x_{Bj} < 0.6$. Almost direct quark/anti-quark separation is possible with forward/backward leptons from W^- production in the PHENIX muon arms due to much larger quark density vs anti-quark density at large momentum transfer. In this case, $A_L(\text{forward } W^- \rightarrow \mu^-) \approx \Delta d/d$. Similarly, $A_L(\text{backward } W^- \rightarrow \mu^-) \approx \Delta \bar{u}/\bar{u}$. Additionally, measurement of W^+ production will give access to $\Delta u/u$ and $\Delta \bar{d}/\bar{d}$. However, due to the fixed neutrino helicity, the flavor contributions in forward and backward rapidity are mixed. Similarly, the parity-violating asymmetry of W^+ production in central rapidity combines contributions from both u and \bar{d} polarizations, and from d and \bar{u} polarizations in W^- production. These measurements will have their greatest impact in improving global fits that seek to determine the polarized parton distribution functions in the proton.

Figure 29 shows our expectations, assuming 60% polarization, for the asymmetry uncertainties with 300 pb^{-1} recorded at forward, central, and backward rapidities. The curves refer to various models of quark polarization in the nucleon; work is ongoing to develop an expectation for the uncertainties in the quark polarizations themselves.

5.3 Expectation for Gluon Spin Polarization Measurements

Our main tool, in the short run, for constraining the gluon spin contribution to the proton spin will continue to be $A_{LL}^{\tau^0}$. The three plots shown in Fig. 30 compare our expected

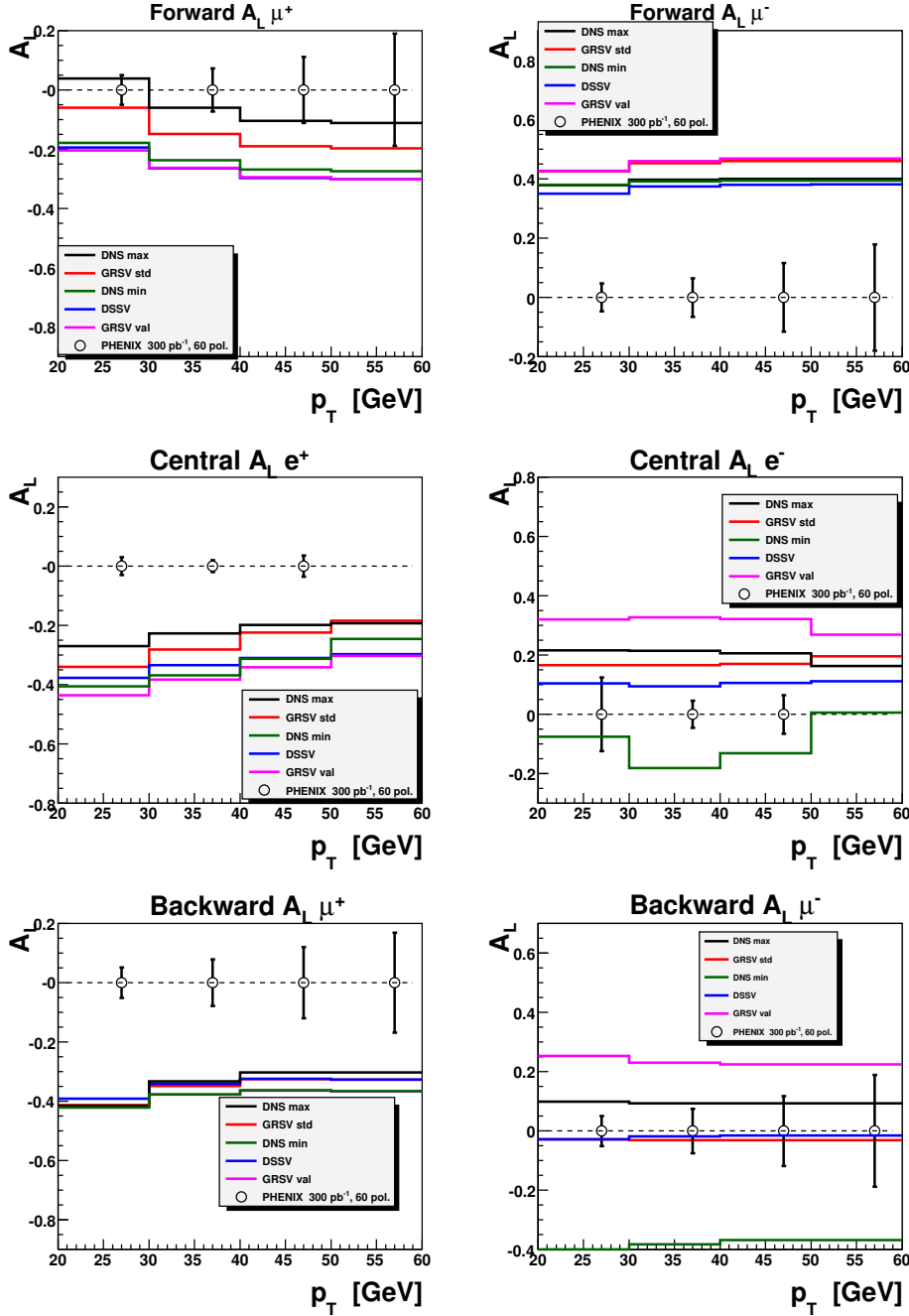


Figure 29: Expectation for uncertainties in W asymmetry measurements with 300 pb^{-1} recorded at (top) forward, (middle) central, and (bottom) backward rapidity. 60% polarization is assumed.

uncertainties in A_{LL}^0 as a function of x_T for 200 GeV (using our expected total after Run-9, 25 pb^{-1}) and for 500 GeV (we expect to reach 50 pb^{-1} recorded in Run-11 and 300 pb^{-1} recorded in Run-14). For 500 GeV running in Run-11 the top two plots in

Fig. 30 show expectations assuming (top left) 50% and (top right) 60% polarization. The two lowest x_T points at 500 GeV, which fall below the lowest x_T points from 200 GeV, will give us sensitivity to $x_g < 0.02$. Comparing the sizes of the uncertainties on those points, it is clear that obtaining 60% polarization or more at 500 GeV makes this program viable. The machine development time we propose for Run-10 would have a primary goal of improving the polarization.

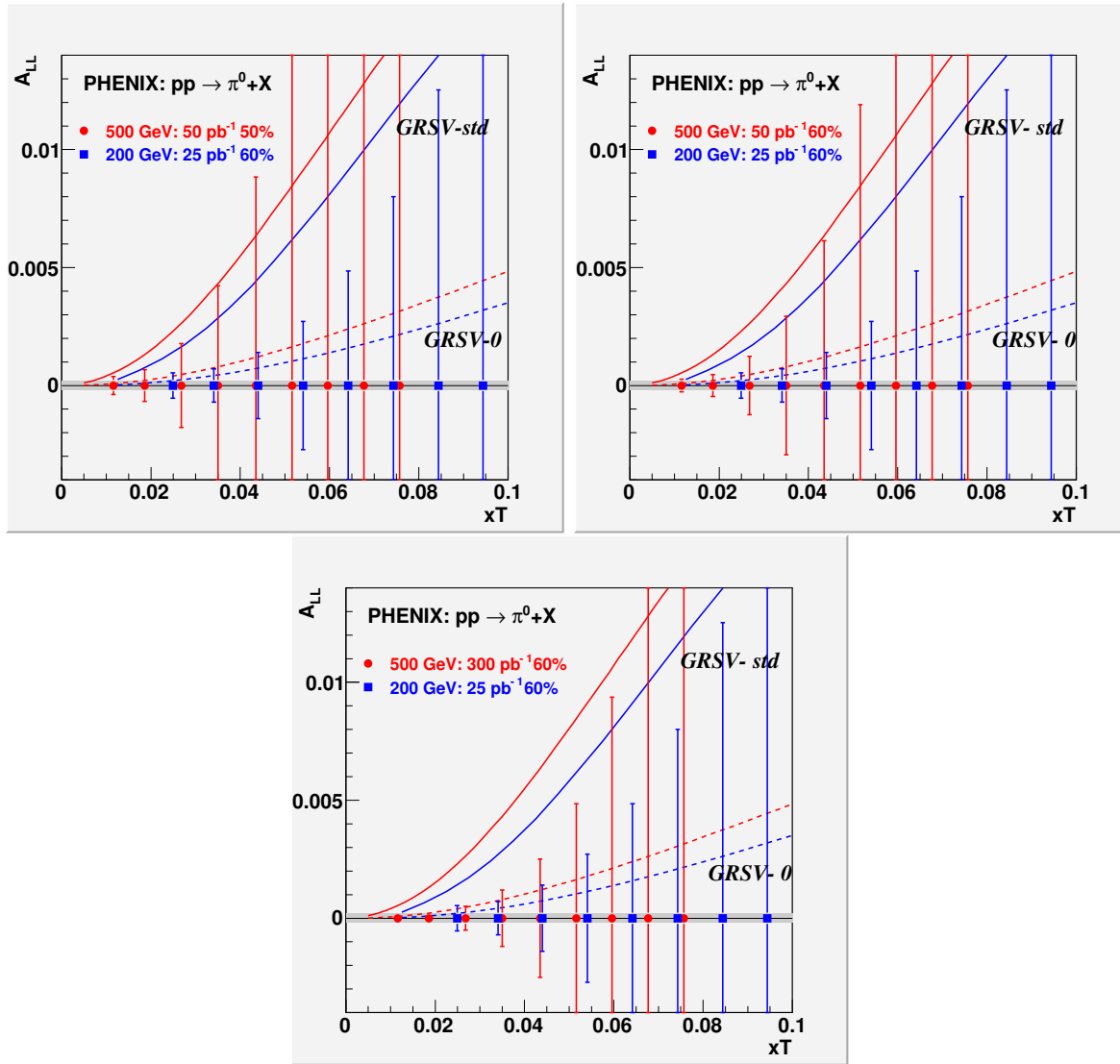


Figure 30: Expected uncertainties in $A_{LL}^{\pi^0}$ as a function of x_T . All three plots show 25 pb^{-1} at assuming 60% polarization at 200 GeV. Also shown for 500 GeV are expectations (top) for 50 pb^{-1} in Run-11 assuming (top left) 50% and (top right) 60% (bottom) for 300 pb^{-1} in Run-14 assuming 60% polarization.

6 Beam Use Proposal for Run-10 and Run-11

6.1 Planning Assumptions and Methodology

The Associate Laboratory Director for Nuclear and High Energy Physics has directed the experiments to plan assuming 25 or 30 weeks of cryo operations in Run-10 and 25 cryo weeks in Run-11.

Detailed guidance provided by the Collider-Accelerator Department (C-A D) describes the projected year-by-year luminosities for various species, along with the expected time-development of luminosity in a given running period[45]. We have used the species-dependent luminosity guidance, the stated cool-down time, and the stated start-up and ramp-up time for each species to convert the required delivered integrated luminosities into a plan for the approximate number of weeks at each species. The by-now extensive experience with operating RHIC in a variety of modes and in understanding luminosity limitations provides confidence in the projected minimum luminosities, which are based on either actual experience or achieving the same charge per bunch as for Au beams. Maximum projected luminosities are based on current understanding of the accelerator limits. As in past beam use proposals, we use the geometric mean of the minimum and maximum projected luminosities. We applaud the C-A D efforts to develop stochastic cooling, and request annual full energy Au+Au runs to support this development, as well as to provide data for our ongoing physics program. Once the EBIS source is fully functional, we look forward to a program utilizing collisions of U+U. However, given the planned EBIS completion date and our need to integrate luminosity for rare probes, we anticipate first U+U running in 2012 (Run-12).

Based on the CA-D guidance [45], we assume the following for luminosities and polarization:

- After the ramp-up period, average Au+Au delivered luminosity per week at $\sqrt{s_{NN}} = 200$ GeV is $495 \mu\text{b}^{-1}$ in Run-10 and $680 \mu\text{b}^{-1}$ in Run-11.
- Based upon the 500 GeV p+p run recently completed, we assume that a goal of 150 pb^{-1} delivered can be reached in 10 weeks. This represents only a small increase over the instantaneous luminosity observed during the last 3 weeks of the 500 GeV run. The integral is attainable with 10 successful stores per week.
- Assuming that the requested machine development of polarization at $\sqrt{s} = 500$ GeV is carried out in Run-10, we present a plan assuming 60% polarization in Run-11.

We determine recorded luminosity from delivered luminosity using a factor of 0.33, which has been observed over the past two years. This factor is dominated by the vertex

cut of +/-30 cm and unusable luminosity at the beginning of a store prior to completion of the high voltage ramp of PHENIX wire chambers. The latter is included in the PHENIX up-time of 70%. Other ingredients in this factor are live-time (90%), trigger efficiency inside the vertex (96% - simulated efficiency for the RXNP trigger down to 10 GeV), offline QA efficiency (85%) and offline vertex cuts (90%).

To estimate luminosities in the energy scan, we assume that the delivered luminosity scales with beam energy squared due to increased emittance, and that the vertex distribution remains unchanged at energies above transition energy where the storage RF can be used. For energies below transition, we correct the projected recorded luminosities for the broadening of the vertex distribution to $\sigma = 150$ cm. We use a correction factor of 0.15/0.5, corresponding to the expected/observed fraction of collisions with vertex inside 30 cm. The resulting rates of events recorded are shown in Table 4. As these event rates are extremely low compared to the maximum event rate that PHENIX can record, we plan to record each minimum bias event and remove non background events offline. Once the energy is well below transition, we will use the VTX detector to separate beam-beam from beam-gas and beam-pipe collisions. This motivates PHENIX to request very low energy running only after the VTX is in operation, and will cause the vertex cut to shrink to +/- 10 cm for all events, regardless of which detectors are used for analysis. For this reason, we propose that very low energy running be scheduled once electron cooling in the AGS is available.

Table 4: Au+Au luminosities and rates expected in Run-10 (**includes ramp-up time for 200 GeV*).

$\sqrt{s_{NN}}$	L/wk del.	L in 4 wks*	L recorded	del. collisions/sec	rec. collisions/sec
200	495 μb^{-1}	1059 μb^{-1}	353 μb^{-1}		
62.4	48.2	192.7	64.2	488	163
39	18.8	75.3	25.1	191	64
27	9.0	36.1	3.61	91	9

6.2 Beam Use Proposal Summary

This proposal aims to maintain the program of discovery physics that has attracted world-wide attention to the RHIC heavy ion program, *while maintaining* progress in the spin physics program and development of polarized proton performance. The PHENIX philosophy is that this is best accomplished by

- a Continued enrichment of existing data sets that are statistically sparse in essential physics channels (which requires accumulation of data over multi-year periods)

- b Optimizing the RHIC run plan to take advantage of key detector upgrades as they become available.
- c Targeting physics goals to utilize RHIC luminosity and ion source improvements in both the heavy ion and spin programs. This consideration is also critical running below injection energy.
- d Continued development of luminosity and polarization for decisive measurements with polarized protons.
- e *Completing* surveys by securing requisite baseline data in a timely fashion, so that comparison data sets are obtained with essentially the same detector configuration.

Table 5: The PHENIX Beam Use Proposal for Runs 10-11.

RUN	SPECIES	$\sqrt{s_{NN}}$ (GeV)	PHYSICS WEEKS	$\int \mathcal{L} dt$ (recorded)	p+p Equivalent
10	Au+Au	200	10	1.4 nb ⁻¹	56 pb ⁻¹
	Au+Au	62.4, 39, 27	10		
	p+p	500	4		
	p+p	22.4	1		
11	p+p	500	10	50 pb ⁻¹	50 pb ⁻¹
	Au+Au	200	8	1.4 nb ⁻¹	56 pb ⁻¹

Table 5 summarizes the current PHENIX Beam Use Proposal.

The requested sequence of runs is motivated by and coordinated with the program of upgrades. In particular, Run-10 will provide the low-mass dilepton physics made possible by the HBD. Following this, commissioning of the VTX detector will begin, leading to separated charm and bottom physics in 2011. Addition of the FVTX in 2012 will allow PHENIX to perform the long awaited quarkonium spectroscopy measurements to probe color screening in the medium. We anticipate beginning the study of U+U collisions at that time, as well. It should be noted that the need for equivalent p+p integrated luminosity to provide adequate baseline data for the heavy ion program will provide additional data toward our goals for spin measurements at 200 GeV.

6.3 Run-10

The highest priority for the PHENIX Collaboration in Run-10 is to record 1.4 nb⁻¹ of 200 GeV Au+Au collisions, utilizing the Hadron Blind Detector to reject Dalitz decays and

conversion electrons. This will require 10 weeks of Physics running, assuming RHIC performance midway between the projected minimum and maximum luminosity. This data set will provide low mass dilepton spectra of sufficient precision to search for modification in medium of ρ , ω and ϕ meson spectral functions. The systematic and statistical uncertainties in the low-mass dilepton enhancement observed by PHENIX will be substantially reduced. Furthermore, a data sample of 1.4 nb^{-1} will be twice the size of the one collected in Run-7. Addition of this new data set will allow measurement of the upsilon suppression factor, replacing the current upper limit. It will also increase the kinematic range of gamma-hadron, di-hadron, reconstructed jet, non-photon electron flow and baryon spectra measurements.

PHENIX will install the silicon vertex detector prior to Run-11. As the Hadron Blind Detector and the Reaction Plane Detector cannot coexist with the silicon vertex detector, it is imperative to collect data with the HBD in Run-10. Furthermore, the non-photon electron flow statistics must be collected in Run-10 in order to make use of the excellent reaction plane resolution of the RXNP detector.

Our second priority in Run-10 is to begin an energy scan, focusing first between full and injection energies. PHENIX proposes this approach in large part due to practical considerations. The first consideration is that Run-10 provides a unique opportunity to investigate dielectron production in a completely new collision energy regime while the HBD is in place. Measurement at two intermediate energies will allow observing how the dilepton excess and rho modification observed at the SPS expands into the large excess at very low mass observed at $\sqrt{s}=200 \text{ GeV}$. New analysis techniques suggest a way to measure the spectral function in the continuum region. This is very promising, as it can be related to the charge correlator in the medium and can be calculated theoretically. Utilization of the HBD to reject background will allow PHENIX to carry out this measurement with 50 Million events, reducing the required running time by a factor of 6. Without this reduction, the required running time is prohibitive. With the HBD, dielectron production can be studied at 39 and 62.4 GeV.

The second practical consideration is that the collision rates below injection energy become extraordinarily low due to the E^2 scaling of collider luminosities and filling of the time bucket by beam particles when the energy is too low to allow use of the storage RF. Operation at 1 Hz or less is poorly matched to the PHENIX optimization for rare probes. However, the large acceptance of the new silicon vertex detector, coupled with a new start time and trigger detector, will allow much more efficient operation of PHENIX at low \sqrt{s} and low collision rate. These will allow a compelling program of measurements of hadronic and fluctuation observables at low \sqrt{s} . A new start/trigger detector is under discussion within the collaboration; construction is foreseen to require approximately 12 months. The excellent VTX pointing resolution is expected to allow clean separation of beam-beam from beam-gas and beam-pipe interaction. Consequently, PHENIX proposes that runs below injection energy be performed in 2012 or later. Furthermore, we would

like to see the timing of this part of the low energy scan matched to construction of electron cooling in the AGS. Boosting the collision rate will significantly improve the operational efficiency at low energies.

PHENIX proposes to record 350 million, 50 million and 25 million minimum bias Au+Au collisions at $\sqrt{s}=62.4, \approx 39$, and 27 GeV, respectively. We anticipate that this will require 3.5 weeks at 62.4 GeV, 1.6 weeks at ≈ 39 GeV and 4.5 weeks at 27 GeV. The exact energy near 39 GeV should be chosen such that the storage RF is operable, as the collision rate that can be recorded by PHENIX otherwise decreases by a factor of 3.3 due to the longer collision vertex without storage RF.

This program will allow measurement of dielectrons at the two higher energies, and a search for the onset of perfect liquid properties by measurement of the opacity of the produced medium and elliptic flow at all three energies. Opacity to light quarks will be determined from $\pi^0 R_{AA}$ at all three energies, and for heavy quarks at 62.4 GeV. p+p comparison yields will be initially determined via the parameterization of d'Enterria [39], pinned to a new measurement by PHENIX at 22.4 GeV as proposed below. Elliptic flow of identified hadrons will be measured to sufficiently high p_T to identify the point where quark number scaling breaks at the two highest energies. The p_T dependence of inclusive hadron elliptic flow will be measured at all three energies with sufficient precision to constrain to viscosity to entropy ratio by comparison to calculations with viscous hydrodynamics. Equally importantly, the same data sets will be used to search for possible evidence of the QCD critical point in the lower part of the μ range predicted by various lattice calculations. This search will utilize v_2 , fluctuations, HBT correlations, and identified hadron yield observables.

Our third priority for Run-10 is a period of approximately 5 weeks of p+p collisions. We request that up to 4 weeks be devoted to machine development studies in order to improve the proton polarization in 250 GeV beams and reduce backgrounds. This machine development time is key to the success of the spin program from 2011 onwards. The remaining week should be devoted to unpolarized proton-proton collisions at 22.4 GeV to serve as reference for the existing Cu+Cu data at that energy. This data will replace the existing reference spectrum, which was created by combining results from multiple ISR experiments and suffers from large systematic uncertainties. Reducing the error bars will pin down the R_{AA} at 22.4 GeV and provide the means for interpolation of p+p spectra to serve as reference for 39 and 27 GeV Au+Au data. In order to match the uncertainties in the π^0 spectrum in heavy ion collisions, 2.5 billion p+p events should be sampled. This should require approximately one week of RHIC running time, including the energy change time.

Table 6: Detailed plan for Run-10.

	$\sqrt{s_{NN}}$	weeks	events	comment
cooldown		2		
Au+Au start/rampup	200	3		
Au+Au physics	200	10		record 1.4nb^{-1}
	62.4	3.5	350M	
	≈ 39	1.6	50M	
	27	4.5	25M	
p+p development	500	4		PHENIX ops as needed
p+p physics	22.4	1	2.5B	
warm-up		0.5		
TOTAL		30		

6.4 Run-11

By Run-11, the PHENIX central barrel silicon vertex detector (VTX) will be completed and installed. Consequently, we request p+p collisions to further the goals of the spin program, followed by full energy Au+Au collisions to make first measurements of charm and bottom separately. In addition to the first VTX running opportunity, Run-11 will see the majority of the muon trigger upgrade installed. PHENIX will have in place all Muon tracker FEE components, and RPC3's in both arms. This leaves us with full functionality for the online W trigger. RPC1 installation will be done in the shutdown following Run-11. The RPC1's will provide additional timing information and improve the offline background rejection, particularly of cosmics. However, even without this, a first W asymmetry physics run is feasible with good performance.

The highest priority for PHENIX in Run-11 is polarized proton running to make progress toward our spin physics goals. It is the conclusion of the collaboration that RHIC has reached the realm of diminishing returns running at 200 GeV at current luminosity levels. The smallness of both ΔG and the achieved and projected luminosities mean that a significant improvement upon the Run-9 data set is unlikely. At high luminosity, the possibility of measuring direct photon A_{LL} is promising, but applying approximately half of Run-11 to this would produce a result of potentially marginal utility. Consequently, PHENIX request 50 pb^{-1} recorded (150 pb^{-1} delivered) of 500 GeV polarized proton collisions. The required polarization is 60%; we request this goal under the assumption of successful polarization development in Run-10. We estimate 10 weeks of physics running will be required to reach this goal. In parallel with key physics measurements, this run will allow commissioning of the VTX.

The physics delivered with this first 500 GeV production run is two-fold, and described in detail above. We will make the first W asymmetry measurement to look at light quark

and anti-quark polarization. And, we will measure ΔG via midrapidity π^0 A_{LL} . The two lowest x points at 500 GeV fall below the lowest x points in the 200 GeV data, extending our sensitivity down to $x < 0.02$.

The second priority to record 1.4 nb^{-1} in a vertex cut of ± 30 cm. This data set, albeit the subset inside 10 cm, will provide a first measurement of separated open charm and bottom energy loss and flow, utilizing the VTX. The data set into the full vertex range will provide sufficient statistics, when combined with Run-10 and Run-7, for a definitive measurement of J/ψ v_2 .

References

- [1] Initial PHENIX Run-1 request, 24-May-99,
<http://www.phenix.bnl.gov/phenix/WWW/publish/za jc/sp/presentations/RBUP99/rbup99.htm>
- [2] PHENIX Run-1 presentation to PAC, 23-Mar-00,
<http://www.phenix.bnl.gov/phenix/WWW/publish/za jc/sp/presentations/RBUP00/rbup00.htm>
- [3] PHENIX Run-2 presentation to PAC,
<http://www.phenix.bnl.gov/phenix/WWW/publish/za jc/sp/presentations/RBUP-Nov00/RBUPNov00.htm>
- [4] PHENIX Run-2 proposal for extended running:
<http://www.phenix.bnl.gov/phenix/WWW/publish/za jc/sp/presentations/RBUPSep01/RBUPSep01.html>
- [5] PHENIX Runs 3-5 proposal to PAC, Aug-02,
<http://www.phenix.bnl.gov/phenix/WWW/publish/za jc/sp/presentations/RBUP-PAug02/RBUPforAug02PAC.pdf>
- [6] PHENIX Beam Use Proposal for RHIC Runs 4-8, Sep-03,
<http://www.phenix.bnl.gov/phenix/WWW/publish/za jc/sp/presentations/RBUP03/ProposalText/RBUPforRuns4-8.pdf>
- [7] PHENIX Beam Use Proposal for RHIC Runs 5-9, Jul-04,
<http://www.phenix.bnl.gov/phenix/WWW/publish/za jc/sp/presentations/RBUP04/ProposalText/RBUPforRuns5-9.pdf>
- [8] PHENIX Beam Use Proposal for RHIC Run-6 and Beyond, Oct- 05,
<http://www.phenix.bnl.gov/phenix/WWW/publish/za jc/sp/presentations/RBUP05/ProposalText/RBUPforRun7andBeyond.pdf>

- [9] PHENIX Beam Use Proposal for RHIC Run-7 and Beyond, Sep- 06,
<http://www.phenix.bnl.gov/phenix/WWW/publish/zajc/sp/presentations/RBUP06/ProposalText/RBUPforRun7andBeyond.pdf>
- [10] PHENIX Beam Use Proposal Update for RHIC Run-7 and Beyond, Mar-07,
<http://www.phenix.bnl.gov/phenix/WWW/publish/jacak/sp/RBUP07/RBUP07.update.pdf>
- [11] PHENIX Beam Use Proposal for RHIC Run-9 and Beyond, April- 08,
http://www.phenix.bnl.gov/phenix/WWW/publish/jacak/sp/BeamUse08/RBUP08_proposal.pdf
- [12] Research Plan for Spin Physics at RHIC, submitted to U.S. Department of Energy February, 2005, available from <http://spin.riken.bnl.gov/rsc/report/masterspin.pdf>
- [13] Plans for the RHIC Spin Physics Program, submitted to U.S. Department of Energy June, 2008; available from http://spin.riken.bnl.gov/rsc/report/spinplan_2008/spinplan08.pdf
- [14] A. Adare *et al.* (PHENIX Collaboration), arXiv:0903.3399, submitted to Phys. Rev. C (2009).
- [15] A. Adare *et al.* (PHENIX Collaboration), arXiv:0903.4886, submitted to Phys. Rev. C (2009).
- [16] A. Adare *et al.* (PHENIX Collaboration), arXiv: 0903.4851, submitted to Phys. Rev. Lett. (2009).
- [17] A. Adare *et al.* (PHENIX Collaboration), Phys. Lett. B670, 313 (2009).
- [18] A. Adare *et al.* (PHENIX Collaboration), Phys. Rev. D79, 012003 (2009).
- [19] A. Adare *et al.* (PHENIX Collaboration), arXiv:0810.0694, accepted in Phys. Rev. Lett. (2008).
- [20] Daniel de Florian, Rodolfo Sassot, Marco Stratmann and Werner Vogelsang, arXiv:0804.0422 (2008).
- [21] B. Jäger *et al.* Phys. Rev. **D67**, 054005 (2003); M. Glück *et al.*, Phys. Rev. **D63**, 094005 (2001).
- [22] A. Adare *et al.* (PHENIX Collaboration), arXiv:0804.4168, submitted to Phys. Rev. Lett. (2008).
- [23] A. Afanasiev *et al.* (PHENIX Collaboration), arXiv:0903.4863, submitted to Phys. Rev. Lett. (2009).
- [24] A. Adare *et al.* (PHENIX Collaboration), Phys. Rev. **C** 78, 044902 (2008).

- [25] A. Afanasiev *et al.* (PHENIX Collaboration), arXiv:0905.1070, submitted to Phys. Rev. C (2009).
- [26] Jorge Casalderrey-Solana and Derek Teaney, Phys. Rev. D **74**, 085012 (2006).
- [27] W.A. Horowitz and M. Gyulassy, arXiv:0706.2336 (2007).
- [28] K. Adcox *et al.* (PHENIX Collaboration), Nucl.Phys. **A757**, 184 (2005).
- [29] A. Adare *et al.* (PHENIX Collaboration), Phys. Rev. Lett. **98**, 172301 (2007).
- [30] A. Adare *et al.* (PHENIX Collaboration), Phys. Rev. C **77**, 064907 (2008).
- [31] A. Adare *et al.* (PHENIX Collaboration), Phys. Rev. Lett. **101**, 232301 (2008).
- [32] I. Vitev, Phys. Lett. **B639**, 38 (2006).
- [33] S.S. Adler *et al.* (PHENIX Collaboration), Phys. Rev. Lett. **94**, 232302 (2005).
- [34] L.P. Csernai, J.I. Kapusta and L.D. McLerran, Phys. Rev. Lett. **97**, 152303 (2006).
- [35] V. Nosenko and J. Goree, Phys. Rev. Lett. **93**, 155005 (2004).
- [36] P. Coleman and A. J. Schofield, arXiv:cond-mat/0503002, published in Nature 4333, 226 (2005).
- [37] S.A. Hartnoll, C.P. Herzog and G.T. Horowitz, Phys. Rev. Lett. **101**, 031601 (2008).
- [38] K. Rajagopal, “Can We Discover the QCD Critical Point at RHIC?,” RHIC 2006 Critical Point Workshop, <https://www.bnl.gov/riken/QCDRhic/talks.asp>.
- [39] F. Arleo and D. d’Enterria, Phys. Rev. D **78**, 094004 (2008).
- [40] S. Afanasiev *et al.* (PHENIX Collaboration), arXiv:0706.3034, submitted to Phys. Rev. Lett. (2007).
- [41] R. Arnaldi *et al.* (NA60 Collaboration), Phys. Rev. Lett. **96**, 162302 (2006).
- [42] Th. Renk, arXiv:0901.2818 (2009).
- [43] H. Zhang, J.F. Owens, E. Wang and X-N. Wang, arXiv:0902.4000 (2009).
- [44] N. Borghini and U. A. Wiedemann, hep-ph/0506218; N. Armesto, L. Cunqueiro, C. A. Salgado and W. C. Xiang, JHEP **0802**, 048 (2008).
- [45] RHIC Collider Projections (FY2009-FY2013), W. Fischer *et al.*, last updated December 29, 2008 available from <http://www.agsrhichome.bnl.gov/RHIC/Runs/RhicProjections.pdf>